Investigation of New 2-Aryl Substituted Benzothiopyrano[4,3-*d*]pyrimidines as Kinase Inhibitors targeting Vascular Endothelial Growth Factor Receptor 2.

Silvia Salerno,[1] Anna Maria Marini,[1*] Giacomo Fornaciari,[1] Francesca Simorini,[1] Concettina La Motta,[1] Sabrina Taliani,[1] Stefania Sartini,[1] Federico Da Settimo,[1] Aída Nelly García-Argáez,[2] Ornella Gia,[2] Sandro Cosconati,[3] Ettore Novellino,[4] Pilar D'Ocon,[5] Anna Fioravanti,[6] Paola Orlandi,[6] Guido Bocci,[6] and Lisa Dalla Via[2].

Dipartimento di Farmacia, Università di Pisa, Via Bonanno 6, I-56126 Pisa, Italy; Dipartimento di Scienze del Farmaco, Università di Padova, Via Marzolo 5, I-35131 Padova, Italy; DiSTABiF, Seconda Università di Napoli, Via Vivaldi 43, I-81100 Caserta, Italy; Dipartimento di Farmacia, Università di Napoli Federico II, Via D. Montesano, 40, I-80131 Napoli, Italy; Departamento de Farmacologia, Universitat de València Av. Vicente Andrés s/n 46100 Burjassot, València, Spain; Dipartimento di Medicina Clinica e Sperimentale, Università di Pisa, Scuola Medica - Via Roma 5, I-56126, Pisa, Italy.

---

* To whom correspondence should be addressed. Phone: +39 050 2219555 Fax: +39 050 2219605. E-mail: marini@unipi.it.

[1]*Dipartimento di Farmacia, Università di Pisa.*

[2]*Dipartimento di Scienze del Farmaco, Università di Padova.*

[3] *DiSTABiF, Seconda Università di Napoli.*

[4]*Dipartimento di Farmacia, Università di Napoli Federico II.*

[5]*Departamento de Farmacologia, Universitat de València.*

[6]*Dipartimento di Medicina Clinica e Sperimentale, Università di Pisa.*

Abstract. Vascular Endothelial Growth Factor (VEGF) pathway has emerged as one of the most important positive modulators of Angiogenesis, a central process implicated in tumour growth and metastatic dissemination. This led to the design and development of anti-VEGF monoclonal antibodies and small-molecule ATP-competitive VEGFR-inhibitors. In this study, we describe the synthesis and the biological evaluation of novel 2-aryl substituted benzothiopyrano-fused pyrimidines **1a-i**, **2a-i** and **3a-i**. The ability of the compounds to target the Vascular Endothelial Growth Factor (VEGF) pathway was determined *in vitro* exploiting the compounds' antiproliferative efficacy against HUVEC cells. The VEGFR-2 inhibition was confirmed by enzymatic assays on recombinant human kinase insert domain receptor (KDR), by cell-based phospho-VEGFR-2 inhibition assays, and by *ex vivo* rat aortic ring tests. The selectivity profile of the best performing derivatives belonging to series **2** was further explored combining modelling studies and additional assays in a panel of human cell lines and other kinases.

Keywords: Tumor angiogenesis, Receptor Tyrosine Kinases, VEGFR, Kinase Inhibitors, Benzothiopyranopirimidines

1. Introduction

Angiogenesis is a physiological process that leads to the formation of new capillaries sprouting or splitting from pre-existing vessels, a requirement necessary for growth and proliferation of solid tumors. [1]. Accordingly, inhibition of this process may reduce vascularization, resulting in antitumor therapies that are supposed to be less toxic for chronic administration, in comparison with conventional chemotherapeutic treatments, and able to maximize the results, while suppressing tumour metastasis [2,3].

The angiogenic process is orchestrated *via* the expression of a range of cell surface and intracellular proangiogenic factors, including the vascular endothelial growth factor (VEGF) family (VEGF-A, VEGF-B, VEGF-C, VEGF-D, VEGF-E). The various members of the VEGF family have overlapping abilities to interact with a set of highly homologous tyrosine kinase receptors (TKRs): VEGFR-1 (Flt-1) and VEGFR-2 (human KDR or murine Flk-1), largely expressed in endothelial cells, and primarily involved in both physiological and pathological angiogenesis. [4,5]. Although the precise role of VEGFR-1 function is still emerging, it seems to act primarily as a decoy receptor, modulating the availability of VEGF for VEGFR-2, which is the principal receptor, through which VEGF exerts its responses in endothelial cells.

In tumour cells, VEGFR-2 is strongly autophosphorylated by increased expression of VEGFs and mediates a serial of mitogenic and survival downstream pathways, including MAPK, P13K or Akt, which are usually hyperactivated in several malignances [6-8].

From the improved understanding of angiogenesis mechanisms in tumorigenesis, the therapeutic strategies blocking VEGF/VEGFR-2 signalling systems became a promising and well-validated approach for suppression of pathological neovascularisation and, consequently, for the treatment of both solid tumours and haematological malignancies [9,

10]. Agents currently developed against VEGF or its receptors include the humanized anti-VEGF monoclonal antibody Bevacizumab, which targets extracellular VEGF. By means of receptor-based virtual screening studies, a significant number of small molecules VEGFR-2 inhibitors, which compete with ATP binding in the catalytic domain of tyrosine kinase, has been developed, leading to the identification of several classes of VEGFR inhibitors, such as Semaxanib (SU5416), Vandetanib (ZD6474), Vatalanib (PTK787), and AAL993 (ZK260253), (Chart 1).

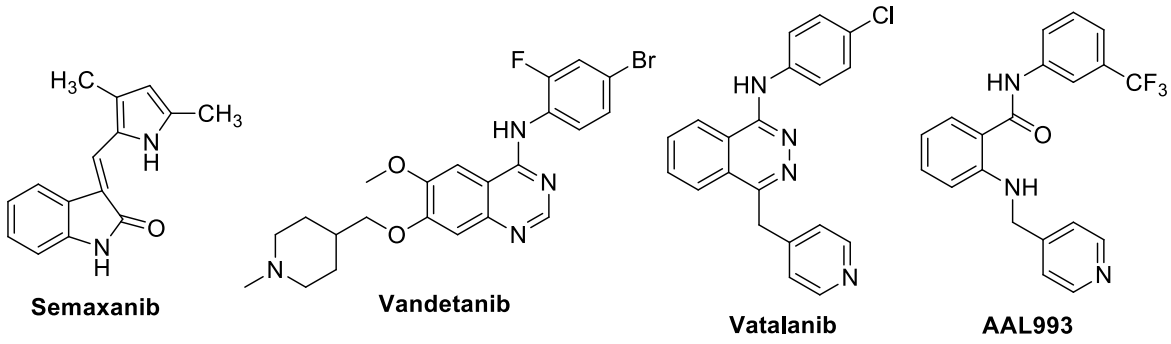

Chart 1. Structures of VEGFR Tyrosine Kinase inhibitors.

The most performing leads, designed as ATP competitive compounds, proved to firmly bind to the catalytic site of the proteins, exploiting hydrophobic interactions, strengthened by one or more hydrogen bonding groups, often heteroatoms. Moreover, other substituents, connected by different spacer chains, including amino and/or amide groups, can protrude toward two other distinct areas of the site: the so called “solvent accessible region” and “buried region” [11, 12].

Among the wide series of thoroughly described chemical structures [13, 14], we drew our attention on those containing, as privileged moiety, a pyrimidine ring, either isolated or fused to form different heterocyclic structures, (Pyrrolo-pyrimidines, Pyrazolo-

pyrimidines, Furo- and Thieno-pyrimidines, Pyrimido-pyrimidinones, Pyrido-pyrimidones) that have been reported as interesting VEGFR inhibitors (Chart 2).

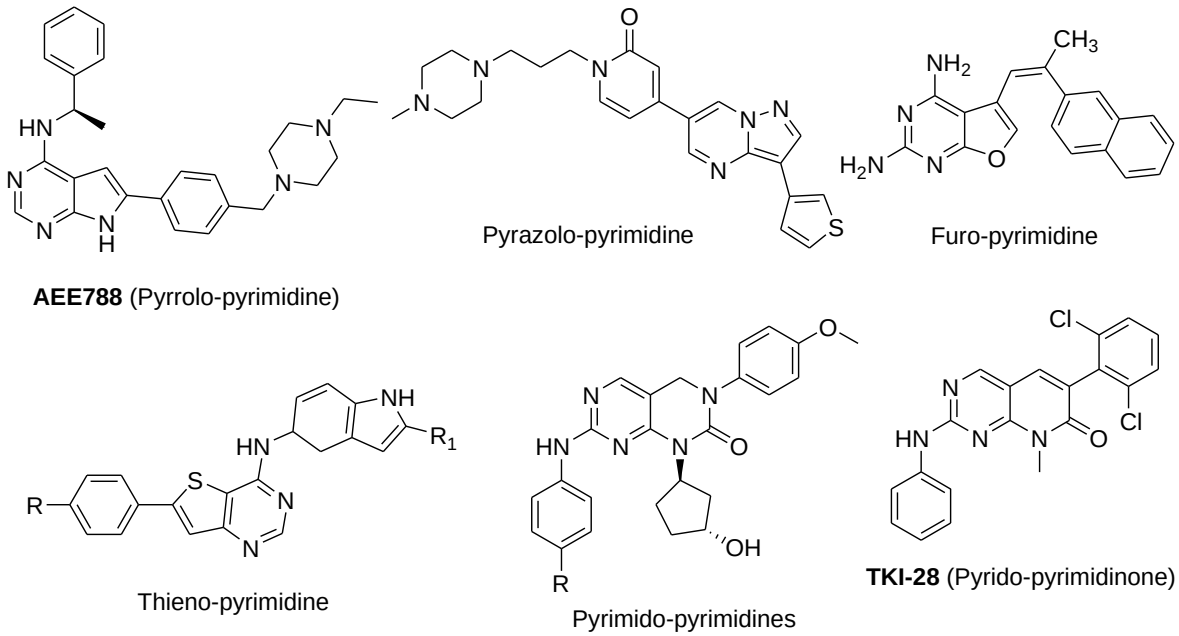

Chart 2. VEGFR inhibitors containing both pendant or fused pyrimidines.

The research program of our group has always been devoted to the preparation and the evaluation of polycyclic chromophores extensively studied as new antiproliferative agents [15-17]. In the last years, some studies on the benzothiopyranopyrimidine system gave rise to the disclosure of novel compounds endowed with interesting pharmacological properties [18,19]; in particular the benzothiopyranopyrimidine **A** (Chart 3) showed an appreciable cytotoxic activity on HL-60 cell line (GI_{50} = 7.15 μM) [20].

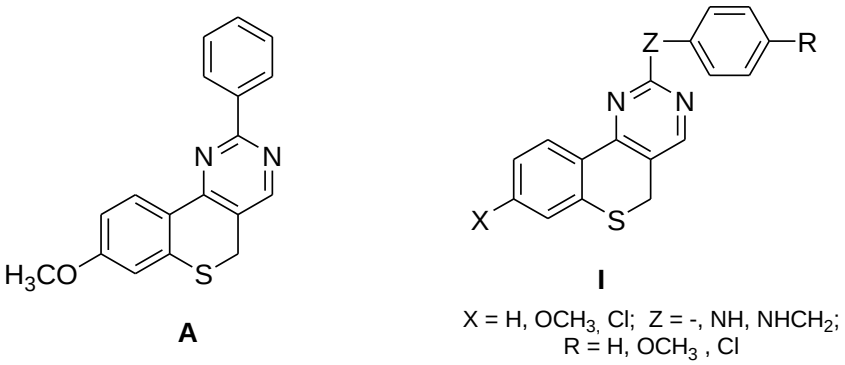

Chart 3. Structures of benzothiopyranopyrimidines.

Focusing on these results and moving from the structures of some reported anilino substituted pyrimidines [21], we designed the series of benzothiopyrano-fused pyrimidines of general formula **I**, (Chart 3), characterized by an aniline moiety inserted in the 2-position of the tricyclic system. Moreover, with the aim to perform critical SAR studies and to confirm the role of the NH group, the analogue 2-benzylamino and 2-phenyl derivatives have been also synthesized.

It was hypothesized that these new products might share the pharmacophoric requirements suitable for an anchoring to the ATP binding site, in particular the aniline NH group and the pyrimidine N_1 and N_3 atoms, that might be implicated in H-bonding interactions with critical residues of the catalytic cleft [13,14].

The ability of the new benzothiopyrano-pyrimidines **I** to inhibit the kinase activity of the VEGFR-2 was determined by a biochemical assay. The effect of the compounds on viability of human umbilical vein endothelial cells (HUVECs) was evaluated by means of an inhibition growth assay. The capacity of the most interesting compounds to inhibit the enzyme catalyzed phosphorylation processes, in HUVECs, as well as the ability to interfere with the angiogenic process *in vitro* on rat aortic rings, has been assayed. The antiproliferative properties of all compounds have been further investigated on a panel of

human tumor cell lines, and the angio-kinase selectivity profile was assessed against a set of 11 human kinases. Finally, molecular docking calculations allowed clarifying at molecular level the interaction pattern established by the compounds with the KDR domain of VEGFR-2.

2. Results and discussion

2.1. Chemistry

The synthetic procedure leading to the target 2-aryl-substituted-5*H*-benzothiopyrano [4,3-*d*]pyrimidine derivatives **1a-i**, **2a-i** and **3a-i** takes advantage by the use as "synthetic tool" of the 7-substituted benzothiopyrane moiety, which was demonstrated to be a versatile intermediate [20].

The 1,3-bielectrophile reactivity of the opportune intermediate 7-substituted-3-dimethylaminomethylene derivatives **4a-c** [20,22-24] in the reaction with the appropriate binucleophile amidines **5a-c** or **6a-c** in an ethanolic refluxing solution, in the presence of sodium ethoxide [25], allowed to easily obtain the desired 2-phenyl substituted pyrimidines **1a-i** and their benzylamino substituted analogues **3a-i**, as reported in Scheme 1. *P*-substituted benzamidine hydrochlorides **5b-c**, even commercially available, were difficult to find; so they were obtained with good yields by reaction of the appropriate benzonitrile derivative with a methanol solution of sodium methoxide and ammonium chloride, as reported in literature [26-28]. The *p*-substituted benzylguanidines **6a-c** were synthesized by condensation of methylthiopseudourea sulfate with the appropriate benzylamine in aqueous solution, following already described procedures [29-31].

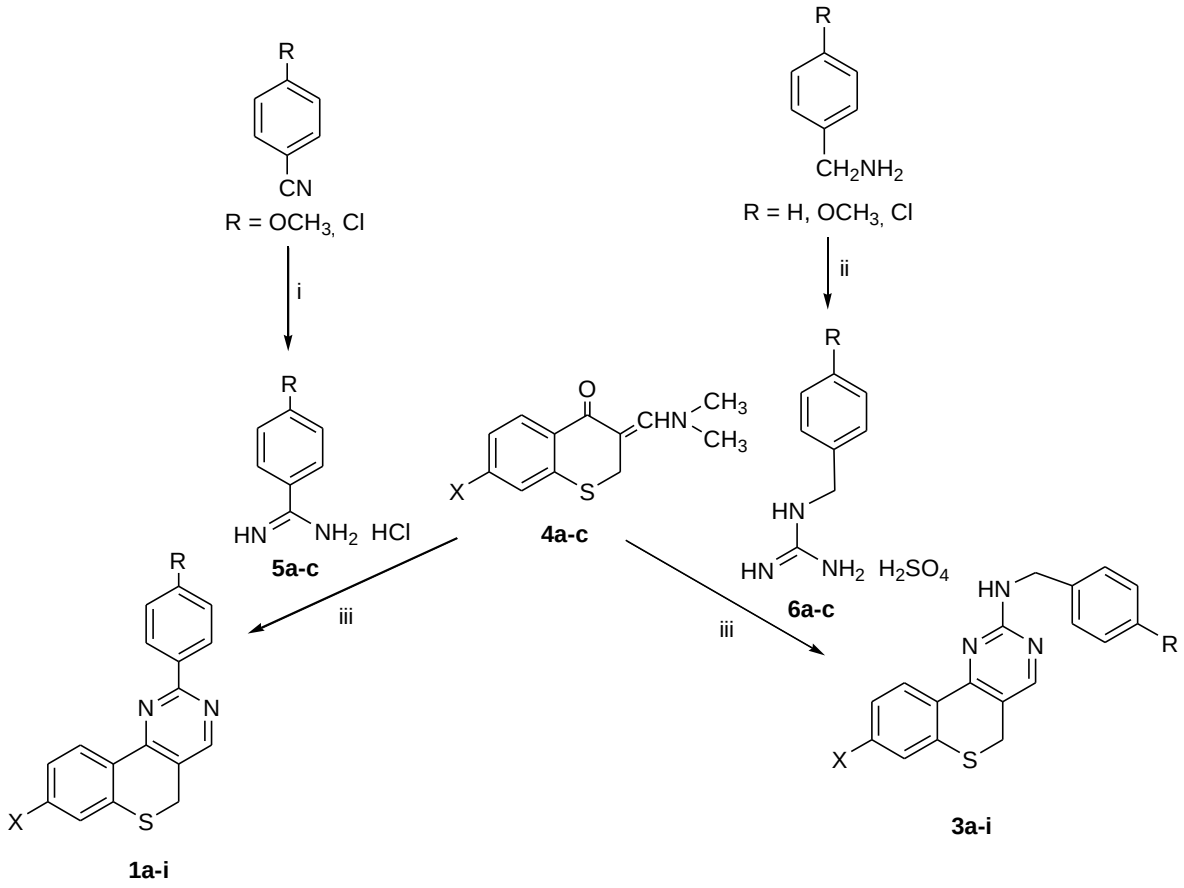

Scheme 1. Reagents and conditions: i) MeONa, MeOH, NH_4Cl; ii) methylthiopseudourea sulphate, H_2O, r.t. for 7 hours, 100 °C for 16 hours; iii) EtONa, refluxing ethanol.

The crude target compounds were obtained as unique products (tlc analysis) in good overall yields, and purified by crystallization.

The preparation of compounds **2a-i** was accomplished by means of a different synthetic route. [32] 3-Dimethylaminomethylene derivatives **4a-c** were allowed to react with guanidine hydrochloride to obtain the 7-substituted-2-aminopyrimidino derivatives **7a-c,** which, by reacting under nitrogen atmosphere with the appropriately *p*-substituted phenyliodide in anhydrous dioxane, in the presence of K_2CO_3, N,N'-dimethylethylendiamine and CuI, afforded the crude target compounds **2a-i** which were

purified by flash chromatography, using petroleum ether 60-80 °C/ethyl acetate 70:30 as the eluting system (Scheme 2).

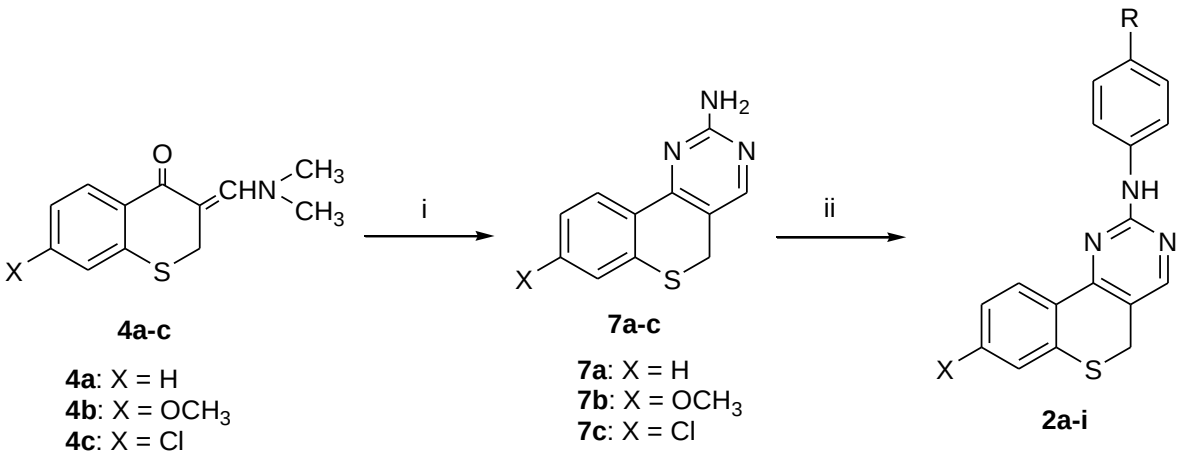

4a-c

4a: X = H
4b: X = OCH_3
4c: X = Cl

7a-c

7a: X = H
7b: X = OCH_3
7c: X = Cl

2a-i

Scheme 2. Reagents and conditions: i) guanidine hydrochloride, EtONa, refluxing ethanol; ii) *p*-substitutedphenyliodide, K_2CO_3, N,N'-dimethylethylendiamine, CuI, dioxane.

The purity of the target compounds was assessed by TLC analysis and by physicochemical properties, analytical and ^{1}H NMR and ^{13}C NMR spectral data, which were in agreement with the proposed structures and with other previously reported results. (Experimental protocols for details).

2.2. Biological evaluation

2.2.1. KDR inhibition assay

The ability of the new 2-aryl-substituted benzothiopyrano-pyrimidines **1a-i**, **2a-i** and **3a-i** in inhibiting the kinase activity of the VEGFR-2 was determined by a biochemical assay performed with a recombinant human kinase insert domain receptor (KDR), using Semaxanib (SU5414) as reference standard. Despite its moderate potency, Semaxanib

shows a useful selectivity in inhibiting VEGFR-1 and -2 tyrosine kinases and VEGF-dependent endothelial proliferation, as compared with novel more potent but multitargeted receptor tyrosine kinase inhibitors, like Sunitinib or Sorafenib [33]. As reported in Table 1, listing activities expressed as inhibition percentage at 7 μM concentration, the results obtained highlighted generally good to high values of KDR inhibition for the most part of the 2-anilino substituted derivatives (compounds of series **2**), in some cases even higher with respect to that exerted by Semaxanib. Both the addition of a methylene spacer (compounds of series **3**) and the deletion of the amino group (compounds of series **1**) reduced the inhibitory efficacy against the target protein, thus clearly indicating a crucial role for the length of the side chain and the NH group.

Table 1. KDR Enzyme Inhibitory Activity and HUVEC Cell Growth Inhibition of Derivatives **1a-i**, **2a-i** and **3a-i**.

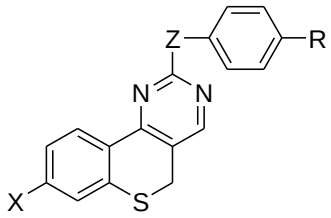

				%[a]	**IC_{50}[b] (μM)**	**GI_{50}[c] (μM)**
Compd.	**Z**	**X**	**R**	**KDR**	**KDR**	**HUVEC**
1a	-	H	H	<20		4.0
1b	-	H	OCH_3	31		12
1c	-	H	Cl	<20		11.3
1d	-	OCH_3	H	<20		2.9
1e	-	OCH_3	OCH_3	<20		4.8
1f	-	OCH_3	Cl	<20		>20
1g	-	Cl	H	<20		2.3
1h	-	Cl	OCH_3	41		4.7
1i	-	Cl	Cl	<20		15.3
2a	NH	H	H	54	8.2	2.4
2b	NH	H	OCH_3	67	2.7	0.45
2c	NH	H	Cl	<20	>50	7.3

2d	NH	OCH_3	H	35	>50	4.3
2e	NH	OCH_3	OCH_3	39	17.5	0.74
2f	NH	OCH_3	Cl	<20	>50	>20
2g	NH	Cl	H	<20	>50	>20
2h	NH	Cl	OCH_3	<20	>50	16.4
2i	NH	Cl	Cl	61	5.6	0.35
3a	$NHCH_2$	H	H	<20		>20
3b	$NHCH_2$	H	OCH_3	<20		>20
3c	$NHCH_2$	H	Cl	<20		12.3
3d	$NHCH_2$	OCH_3	H	<20		>20
3e	$NHCH_2$	OCH_3	OCH_3	<20		>20
3f	$NHCH_2$	OCH_3	Cl	<20		>20
3g	$NHCH_2$	Cl	H	<20		15.1
3h	$NHCH_2$	Cl	OCH_3	35		12
3i	$NHCH_2$	Cl	Cl	<20		17
Semaxanib				40	12.9	13.6

a Percentage of kinase inhibition obtained at 7 μM of test compound.
b IC_{50} values represent the concentration that induces the 50% reduction in enzyme activity.
c GI_{50} values represent the concentration (μM) of compound able to produce 50% cell death with respect to the control culture.

Moreover, an important role of the substituents on both the chromophore and the pendant phenyl moiety, position 8 (X) and 4' (R), was observed. In the case of the 2-anilino-substituted derivatives **2**, when the distal phenyl ring is unsubstituted (**2a, 2d, 2g**), or bears a *p*-methoxy group (**2b, 2e, 2h**), the inhibition percentages progressively decrease when methoxy or, to a greater extent, chlorine substituents are present at 8-position of the chromophore. Conversely, when a pendant *p*-chloro phenyl group is present (**2c, 2f, 2i**) only the insertion of a chlorine in the 8-position, as in compound **2i**, allowed the occurrence of inhibitory capacity. Accordingly, a significant inhibitory efficacy has displayed by compounds **2a**, **2b**, **2e** and **2i**; with **2b** and **2i** showing the highest percentage values in the whole subseries.

Within the series of the 2-phenyl (**1a-i**) or 2-benzylamino (**3a-i**) substituted derivatives, the 8-chloro-4'-methoxy substituted analogues **1h** and **3h** turned out to be the most active inhibitors with percentage values lower or comparable to those of the reference drug.

The activity of the best performing 2-anilino-substituted derivatives was also calculated as IC_{50} (Table 1). The results confirm for **2a**, **2b**, **2e** and **2i** an interesting capacity to inhibit the enzyme, with IC_{50} values ranging from 2.7 to 17.5 μM, comparable (**2e**) or even lower (**2a**, **2b** and **2i**) with respect to that obtained for the reference compound.

2.2.2. Evaluation on HUVEC cells

The ability of new derivatives to inhibit the phosphorylation activity of VEGFR-2, prompted us to test their effect on human umbilical vein endothelial cells (HUVECs) growth by means of an *in vitro* assay. The results, expressed as GI_{50} values, are showed in Table 1, Semaxanib was used as reference compound.

After a 72-h exposure, the ability to exert antiproliferative effects on HUVEC cells was shown by the majority of 2-phenyl substituted pyrimidines **1a-i** showing GI_{50} values, in the micromolar range (from 2.3 to 15.3 μM), comparable or lower to that of Semaxanib. The most part of 2-anilino pyrimidines **2a-i** is able to exert a significant cytotoxicity and, interestingly inside this subseries, derivatives **2b**, **2e** and **2i** show even submicromolar GI_{50} values (0.35-0.74 μM). In contrast, the 2-benzylamino substituted derivatives **3a-i** always exhibited low or null cytotoxic capacities in these cells. Significantly, by comparing the antiproliferative effects exerted by analogous compounds, bearing the same aryl side group, a certain role seems to be played by the substituents in position 8 (X) and 4' (R). Within the sub-series **1a-i,** the most active compounds are **1a**, **1d**, **1g** followed by **1b**, **1e**, **1h**, bearing the unsubstituted (R = H) and the methoxy substituted (R = OCH_3) pendant phenyl group, respectively. Conversely, the presence of a chlorine (R = Cl), as in

compounds **1c**, **1f** and **1i**, generally reduces the activity. As regards the role of the X group in the 8-position, a similar profile is displayed within each group of analogues, since the introduction of methoxy (**1d**, **1e** *versus* **1a**, **1b**) or chlorine (**1g**, **1h** *versus* **1a**, **1b**) increases cytotoxic ability, but in the *p*-chloro subseries (**1f**, **1i** *versus* **1c**). The nature of the substituents X and R also modulates the antiproliferative effects in the group of 2-anilino substituted pyrimidines **2a-i**. Actually, cytotoxic potency is usually enhanced by the insertion of a methoxy electron donating group on the phenyl ring (R = OCH_3, compounds **2b**, **2e** *versus* **2a**, **2d**) or it is lowered by a chlorine (R = Cl, compounds **2c**, **2f** *versus* **2a**, **2d**). The presence of the halogen in the 8-position (X = Cl) on the heterocyclic scaffold gives rise to contrasting results. While 8-chloro substituted pyrimidines have null or scarce activity when R = H (compound **2g**) or R = OCH_3 (compound **2h**), the 4'-chloro analogue **2i** (R = Cl) is surprisingly the most effective to inhibit HUVEC cells growth of the whole series. The less performing was sub-series **3**, actually benzilamino-pyrimidines **3a-i** that displayed comparable and low cytotoxic potencies, independently of the presence of a hydrogen, a methoxy group or a chlorine in the 8 (X) and/or 4' (R) positions. In this latter series of analogues the increase in the distance between the phenyl ring and the amine linker through a methylene spacer seems accountable for the almost disappearance of cytotoxicity, and the dependence of the cellular effects on the other groups appears responsible only for slightly different biological activities.

Overall, the above results confirm the important role played by the NH spacer group, given that only the 2-anilino pyrimidines **2a-i** showed both significant KDR inhibition potency and HUVECs antiproliferative activity, likely correlating the VEGF/VEGFR signal system with their cellular activity.

2.2.3. Inhibition of VEGFR-2 phosphorylation in endothelial cells.

The efficacy observed on HUVEC cells was further investigated by evaluating the ability of the most cytotoxic derivatives, namely **2b**, **2e**, and **2i**, to inhibit the phosphorylation of the target receptor on whole cells [34]. After exposure to **2b** (fig. 1A), **2e** (fig. 1B), and **2i** (fig. 1C) at different concentrations, the amount of the phosphorylated form of VEGFR-2 in HUVEC cell lysates was significantly reduced at the highest concentration (2.5 µM).

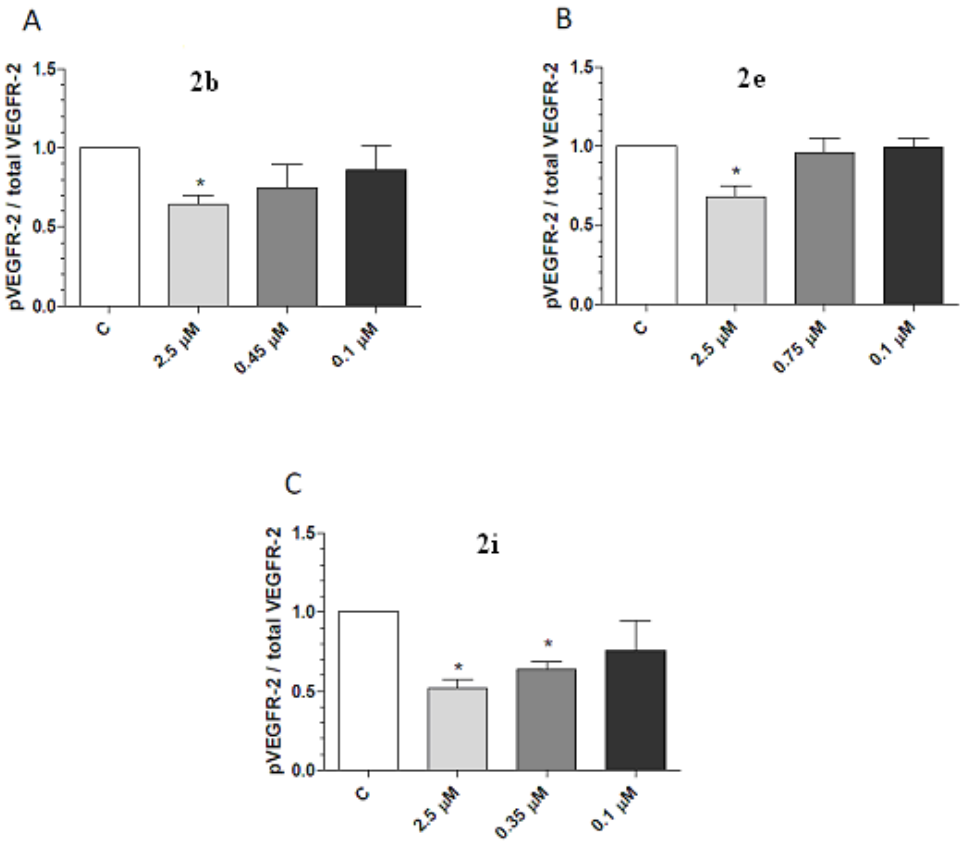

Figure 1. Inhibition of VEGFR-2 phosphorylation by **2b** (**A**), **2e** (**B**) and **2i** (**C**) compounds in HUVEC cells after 72 h of treatment. pVEGFR-2 concentrations were measured by ELISA kits and they were normalized to total VEGFR-2 protein concentration. Columns and bars, mean values ± SD, respectively. **P*<0.05 *vs.* vehicle-treated controls.

In particular, in samples treated with **2b** and **2i** the amount of phosphorylated form of VEGFR-2 significantly decreased in a concentration-dependent manner, starting at the experimental GI_{50} of cell proliferation (figs. 1B and C).

2.2.4. Ex vivo anti-angiogenic activity evaluation

Angiogenesis assays are essential for the identification of potential pro-angiogenic agents as well as for the screening of pharmacological inhibitors. Among them, the *ex vivo* "rat aortic ring" assay, initially developed by Nicosia and Ottinetti [35], bridges the gap between *in vivo* and *in vitro* models. Actually, by using intact vascular explants, the environment in which angiogenesis takes place results more accurately reproduced than that with isolated endothelial cells [36]. Considering that the organization of endothelial cells in capillary-like structures is a process that better occurs in a 3-dimensional extracellular matrix, the culture of rat aortic explants in a matrix of this type results one of the most effective ways for generating new capillaries *in vitro*.

In order to assess their capacity to inhibit microvessel sprouting in an angiogenic process, the selected 2-anilino substituted derivatives **2b** and **2i** have been tested in the *ex-vivo* "rat aortic ring assay". Aortic explants were incubated with compounds **2b** and **2i**, at different concentrations (100 nM, 1 µM, 5 µM and 10 µM) and the activity was compared with that exerted by the reference drug Semaxanib, at the same concentrations, (figs. 2 and 3).

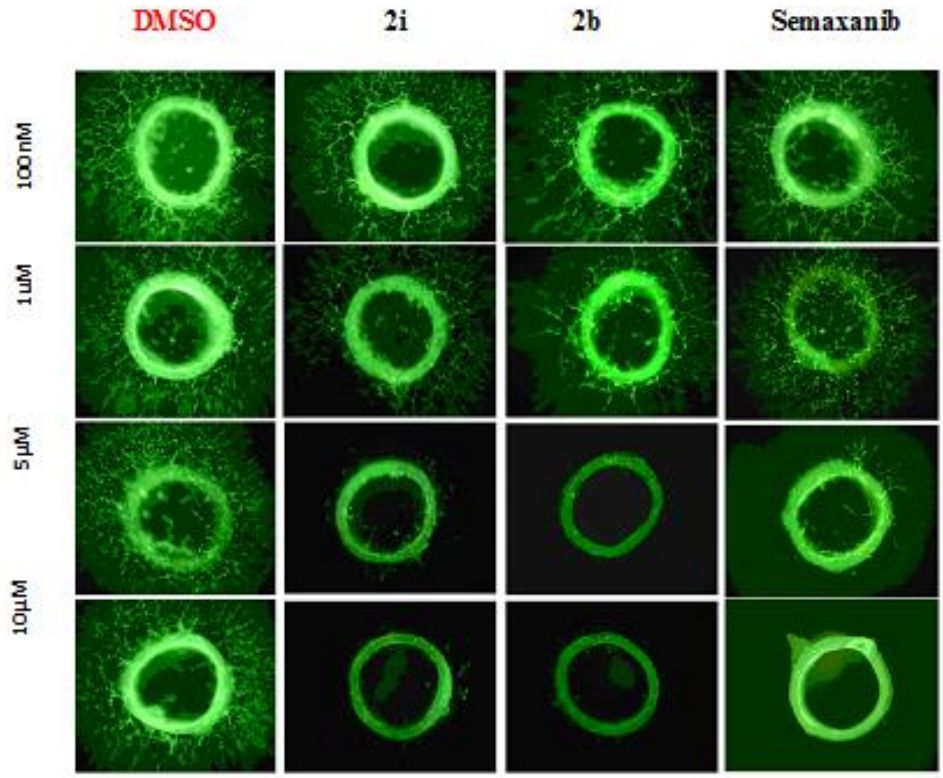

Figure 2. Representative images of the inhibition of microvessel sprouting by compounds **2b**, and **2i** at [100 nM], [1 µM], [5 µM], [10 µM], compared with DMSO and Semaxanib at the same concentrations. Images were visualized using a Nikon fluorescence microscope Eclipse E800 equipped with Nikon camera, with the 4x objective, after fluorescence cell staining at day 7th of the experiment. All experiments have been conducted in duplicate and at least on two different animals.

% INHIB.	2b	2i	Semaxanib
100nM	-8	-0,5	-12
1µM	9	15	-2
5µM	95	88	72
10µM	96	98	100

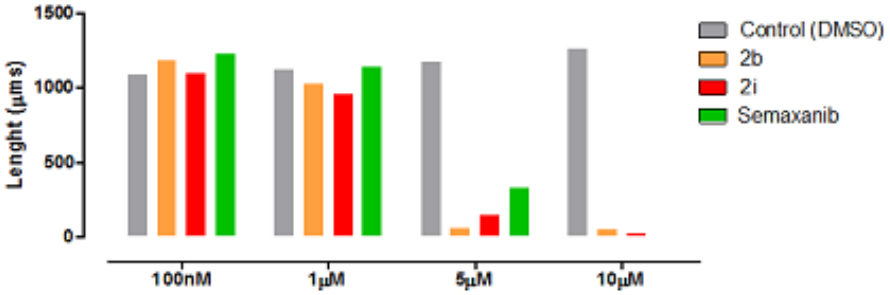

Figure 3. Comparison of the angiogenic growth (Y = Length, µms) of rat aortic explants cultured with compounds **2b** and **2i** at different concentrations (X = 100nM ;1µM; 5µM; 10µM). **DMSO** is used as control and **Semaxanib** as reference compound. Data were calculated at day 7th of the experiment and represent the mean of n = 2-4

Interestingly, both selected compounds inhibit the angiogenic sprouting in aortic ring assay, and the use of different concentrations allowed us to identify the range in which the inhibition took place. In particular, the benzothiopyrano derivatives **2b** and **2i**, seemed to inhibit the process at concentrations ranging from 1 to 5µM, showing a profile similar to that of the reference standard Semaxanib.

2.2.5. Evaluation on HeLa, A-431 and MSTO-211H tumour cell lines

The high structural similarity of kinase ATP binding pocket has made the development of selective inhibitors extremely challenging. Actually, most of the developed angio-kinase

inhibitors also hit a broad range of additional protein kinases; however, a significant capacity to affect simultaneously different mitogenic patways, is often associated with serious side effects and toxicities [37, 38]. In this regard, we studied the cell proliferation profile of the benzothiopyrano collection of compounds **1**, **2** and **3** against a panel of human tumour cell lines expressing different kinases: HeLa (cervix adenocarcinoma), A-431 (epidermoid carcinoma) and MSTO-211H (biphasic mesothelioma). As reported in Table 2, the cell growth evaluation once again revealed a crucial role for the length of the side chain and the presence of the NH group, as evident cytotoxic effects have been observed for the most part of 2-anilino substituted derivatives **2**, showing GI_{50} values in the micromolar range. In addition, a notable effect might also be attributable to the *p*-methoxy substituent on the pendant phenyl ring (R = OCH_3), being **2b** and **2e** the most effective derivatives. The *p*-chlorine (R = Cl) substitution seems to be detrimental, with the exception of **2i** in which, accordingly with the above discussed results, a good activity was present by introducing a chlorine atom on the 8-position (X = Cl).

Table 2. Human Tumour Cell Growth Inhibition of Derivatives **1a-i**, **2a-i** and **3a-i**.

	GI_{50}[a] (μM)		
Compd.	**HeLa**	**A-431**	**MSTO-211H**
1a	>20	>20	>20
1b	>20	>20	>20
1c	>20	>20	>20
1d	>20	6.5±1.2	11.9±1.1
1e	>20	>20	>20
1f	>20	>20	>20
1g	>20	>20	>20
1h	>20	>20	>20
1i	>20	>20	>20
2a	10.2±2.1	>20	11.7±1.3
2b	0.7±0.5	0.96±0.25	1.08±0.04

2c	15.6±2.2	>20	11.5±1.5
2d	20.1	>20	15.0±1.6
2e	0.83±0.14	0.96±0.2	1.08±0.2
2f	>20	>20	>20
2g	>20	>20	>20
2h	2.1±0.2	5.8±0.4	>20
2i	1.5±0.4	2.2±0.4	1.6±0.3
3a	>20	>20	>20
3b	>20	>20	>20
3c	>20	>20	>20
3d	>20	>20	>20
3e	>20	>20	>20
3f	>20	>20	>20
3g	>20	>20	>20
3h	>20	>20	>20
3i	>20	>20	>20

[a] GI_{50} values represent the concentration (μM) of compound able to produce 50% cell death with respect to the control culture.

Between the others subseries, **1a-i** and **3a-i**, only derivative **1d** shows a detectable antiproliferative effect, which appears more significant in A-431 cells.

2.2.6. EGFR inhibition assay

Important evidences point out numerous cross-talks between activated epidermal growth factor receptor (EGFR) largely expressed on A-431 cells and VEGFR [34, 39], moreover a dose-dependent decrease in VEGF expression in EGFR-responsive A-431 cells was indicated for different classes of EGFR targeting agents [40]. Accordingly, the capability of compounds **1d** and **2a-i** to bind EGFR was assayed. The inhibitory effect of the test compounds was routinely estimated at 100 μM, following a previously reported protocol [41, 42]. Compounds **2a-f** displayed null or low percentage values of kinase inhibition, while compounds **1d** and **2g-i** showed a certain capacity to reduce the kinase

activity. These latter compounds, whose percentage values of inhibition were higher than 80%, have been tested at additional concentrations calculating the IC_{50} values, exploiting gefitinib as reference standard (Table 3). Significantly, the shortened derivative **1d** displayed an IC_{50} value of 4.72 μM, in accordance with its antiproliferative activity on A-431 cell line.

Table 3. EGFR Inhibition Data of Derivatives **1d** and **2a-2i**.

Compd.	**EGFR %[a]**	**EGFR IC_{50}[b] (μM)**
1d	100	4.72
2a	50	n.d.[d]
2b	< 50	n.d.[d]
2c	< 50	n.d.[d]
2d	57	n.d.[d]
2e	< 50	n.d.[d]
2f	n. a.[c]	n.d.[d]
2g	100	21.18
2h	93	21.56
2i	81	45.70
Gefitinib		0.022

[a]Percentage of kinase inhibition obtained at 100 μM test compound.
[b] IC_{50} values represent the concentration that induces the 50% reduction in enzyme activity.
[c] not active, [d] not determined

2.2.7. Kinases inhibition assays

The high inhibitory effect of **2b** and **2i** on VEGFR phosphorylation and of **1d** on EGFR kinase activity, prompt us to deepen their kinase selectivity profile. In particular,

their effect has been assessed against a set of 10 human kinases (Akt1/PKBα, AurA/Aur2 kinase, CDC2/CDK1, ERK1, FAK, MEK1/MAP2K1, PDGFRβ kinase, RAF-1 kinase, ROCK1, Src kinase), which are reported to be mainly involved in cell proliferation. No inhibitory activity was detected for **1d** and **2i,** when assayed at 10 μM concentrations (Figs. 4a and 4c), thus excluding any involvement of the tested kinases in the effects of these derivatives on cell viability. Only compound **2b** might appear a multi-target inhibitor of tyrosine kinases, inhibiting besides VEGFR-2, also Aurora kinase and CDC2/CDK1 at significant extent (Fig. 4b).

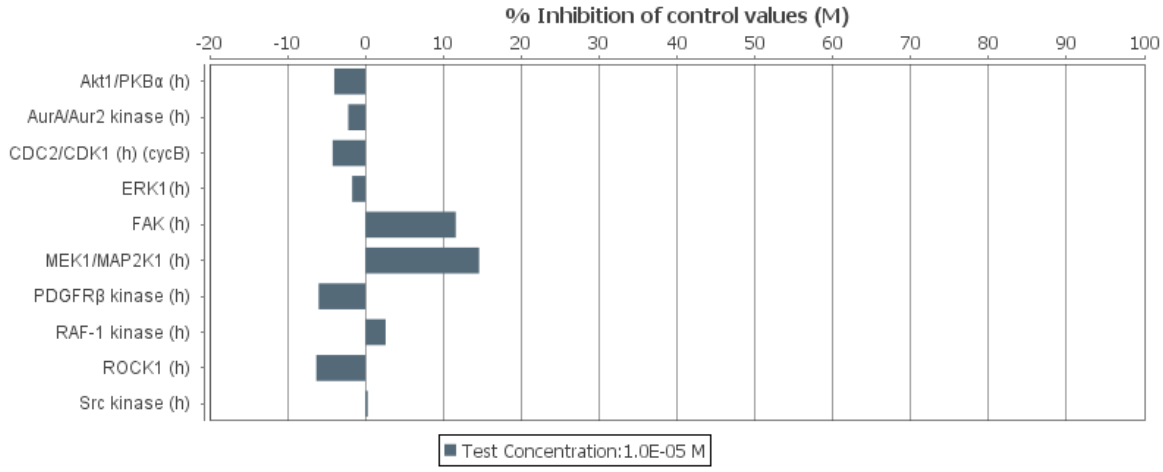

Figure 4a. Kinases Inhibitory Activities of compound **1d**.

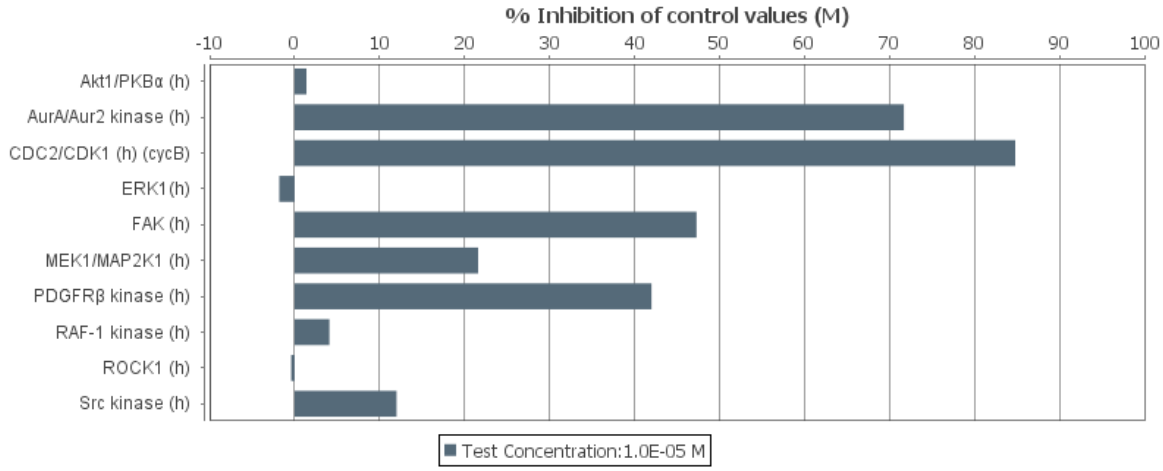

Figure 4b. Kinases Inhibitory Activities of compound **2b**.

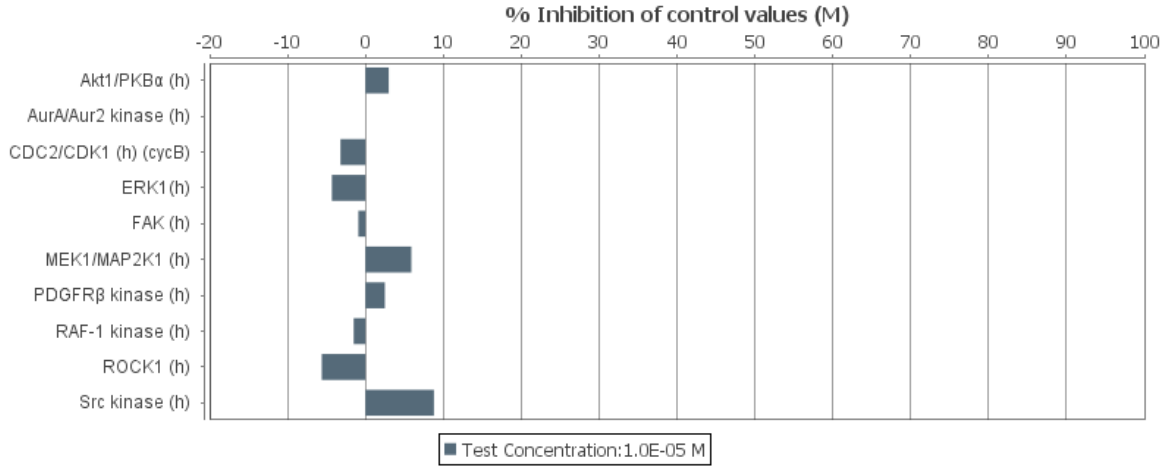

Figure 4c. Kinases Inhibitory Activities of compound **2i**.

2.3. Molecular Modelling

To better understand the reasons behind the VEGFR-2 inhibitory activity of the compounds described above, molecular docking studies were performed on compound **2b.** It displays the highest, although not selective, VEGFR-2 kinase activity inhibitory property (IC_{50} 2.7 μM), high antiproliferative activity on both HUVECs and tumour cell lines

(HeLa, A-431 and MSTO-211H), as well as evident anti-angiogenic properties in the *ex vivo* rat aortic assay.

These calculations were attained using the AD4 software [43, 44]. This choice was dictated by results of a recent work in which this program was demonstrated to be the best in reproducing the experimental (X-Ray) binding pose for different kinases in cross-docking experiments among 17 different docking procedures [45]. To date, more than 30 crystal structures of VEGFR-2 in complex with several inhibitors have been reported. In this inspection, we decided to consider only the structures having a resolution below 2Å (1YWN [46], 2P2H [47], 2XIR, 3BE2 [48], 3EWH [49], 3VHE [50], 3VNT [51], 4AG8 [52], 4ASE [53], 3VO3 [54]) in which 1YWN displayed the so-called A-loop (activation loop) in its open conformation while all the others had the same protein region in its closed form. Among these, the structure 4AG8 was used, as it demonstrated to be the best performing one in AD4 cross-docking experiments. In particular, employing this structure, AD4 was able to reproduce the X-ray conformation of all the analysed co-crystal ligand with an average root-mean squared deviation (rmsd) of 0.89 Å (see Table 4).

Table 4. Rmsd values resulting from cross-docking experiments on the 9 considered VEGFR-2 structures.

		Ligands									
		1YWN	**2P2H**	**2XIR**	**3BE2**	**3EWH**	**3VHE**	**3VNT**	**4AG8**	**4ASE**	**Average rmsd**
Receptors	**1YWN**	0.66	9.55	6.76	0.83	1.16	5.60	6.72	10.66	11.32	5.92
	2P2H	1.57	5.19	10.37	1.48	1.44	1.40	8.72	11.98	8.43	5.62
	2XIR	12.39	11.99	1.90	11.82	2.33	1.72	2.01	1.96	2.19	5.37
	3BE2	3.11	7.97	2.98	1.26	1.03	3.03	6.86	12.83	3.03	4.68
	3EWH	1.17	9.12	2.79	0.90	1.82	2.79	3.19	2.83	2.91	3.06
	3VHE	1.45	11.56	0.85	3.64	0.94	0.83	0.64	0.94	0.79	2.41
	3VNT	10.38	10.75	0.66	1.54	0.95	1.16	0.43	0.46	0.58	2.99
	4AG8	**1.17**	**1.49**	**0.58**	**1.92**	**0.97**	**0.69**	**0.58**	**0.42**	**0.69**	**0.95**
	4ASE	0.89	10.74	0.54	3.06	0.96	0.60	0.39	0.59	0.27	2.01

Interestingly, the 200 independent docking runs of **2b** within the VEGFR-2 kinase active site converged toward a single cluster solution (i.e. binding conformation differing by less than 1.5 Å) for which a binding free energy (ΔG_{AD4}) of -7.62 kcal/mol was predicted (Fig. 5).

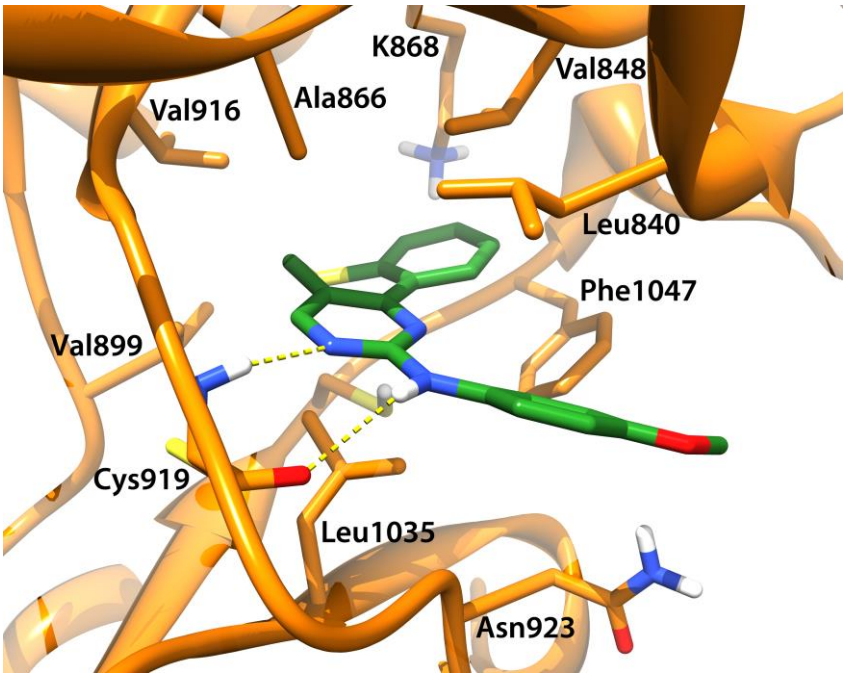

Figure 5. Binding mode of compound **2b,** within the VEGFR-2 active site. The ligand is represented as green sticks while the protein as orange sticks and ribbons. H-bonds are depicted as dashed yellow lines. The picture was rendered with the UCSF Chimera software. [55]

In this conformation, the benzothiopyranopyrimidine scaffold is inserted in the enzyme active site with its nitrogen in position 3 and the adjacent exocyclic NH in position 2 establishing a double H-bond with the backbone NH and CO of Cys919 in the enzyme hinge region, respectively. These interactions explain why **2b** and its closely related congeners are effective VEGFR-2 inhibitors and why the 2-aryl analogues (**1a-i**), by lacking the double H-bond interaction generally display lower inhibition against the enzyme (Table 1). Moreover, the lipophilic benzothiopyranopyrimidine ring is fitting in the hydrophobic ATP cleft where favorable contacts are established with Leu1035, Val899, Val916 (gate-keeper residue), Val848, and Leu840. The limited extension of this cleft would not allow to easily host bulky substituents in position 8 of the chromophore without a subsequent relocation of the ligand. Indeed, this relocation would result in the

loss of the double H-bond interaction with the enzyme's hinge region residues, thus explaining the lower inhibition potencies of compounds **2d-2h**. On the other hand, the presence of the positively charged K868, within the same cleft, should negatively affect the ligand/enzyme recognition suggesting that modifications of the benzothiopyranopyrimidine scaffold, aimed at minimizing these unfavourable contacts, should enhance the inhibitory potencies against the enzyme. We are now testing this hypothesis and results will be reported in due of course. In the binding site, Phe1047 is placed between the benzothiopyrane aromatic ring and the aniline moiety in position 2 of the tricyclic system establishing with them charge-transfer interactions. In this respect, it could be speculated that the double substitution in position 8 (X) and 4' (R) with the electron withdrawing chlorine atom would enhance the strength of the aforementioned interaction thereby explaining why **2i** is still so efficient as VEGFR-2 kinase inhibitor.

The aniline substituent is partially solvent exposed and this should explain why its substitution with the longer 2-benzylamino group would result in weaker VEGFR-2 inhibitors (**3a-i**). As depicted in Figure 5, the *p*-methoxy substituent of **2b** is pointing towards Asn923 residue and in principle additional H-bond interactions could be established through the rearrangement of this residue.

3. Conclusions

Activation of the "angiogenic switch" is considered one of the most critical factors for tumour growth and progression, and numerous small molecule inhibitors of the VEGF-VEGFR pathways have been proven to be an attractive approach for anticancer drug discovery.

In this work, we developed novel antiangiogenic agents based on the benzothiopyrano[4,3-*d*]pyrimidine scaffold, characterized by a pendant aryl moiety. In particular, the synthesis of new benzothiopyrano[4,3-*d*]pyrimidines carrying phenyl (compounds **1a-i**), phenyl-amino (compounds **2a-i**) and benzyl-amino (compounds **3a-i**) side groups in the 2-position of the heterocyclic system is described. Of these derivatives, compounds **2a-i** emerged as the most interesting, revealing that the presence of the anilino side moiety is required to obtain a significant effect against the target proteins.

Compounds **2a-i** displayed a promising inhibitory profile on both human kinase receptor KDR and endothelial HUVEC cells, with values in the low micromolar range**.** The kinase inhibitory activities of the best performing compounds **2b** and **2i** was further investigated by measuring the formation of newly phosphorylated substrates *via* a cell-based phospho-VEGFR-2 inhibition assay. Moreover, their capacity to inhibit the generation of new capillaries was confirmed by means of the *ex-vivo* "rat aortic ring assay".

To determine the compounds' selectivity profile, we evaluated the cytotoxic effects of **1a-i**, **2a-i** and **3a-i** against three human tumour cell lines. As a general trend, only few compounds, belonging to the subseries **2,** retained cytotoxic activity, albeit with about a 2-fold increase in GI_{50} values with respect to HUVECs. Hence, in order to investigate the involvement of other structurally related kinases in the cellular activity, we assayed the capacity of compounds **2b** and **2i** to interfere with a panel of eleven additional human kinases, (EGFR, Akt1/PKBα, AurA/Aur2, CDC2/CDK1, ERK1, FAK, MEK1/MAP2K1, PDGFRβ, RAF-1, ROCK1 and Src kinase). By this study, the most selective derivative seems to be **2i**, conversely, the best performing compound **2b** exhibited a certain activity also against Aurora kinase and CDC2/CDK1, probably due to the high structural similarities shared by the VEGFR-2 ATP binding pocket with that of other kinases.

Molecular docking calculations allowed understanding the interaction pattern established by the compounds and the KDR domain of VEGFR-2. The model, exploited for compound **2b**, showed that the benzothiopyranopyrimidine scaffold could interact with the enzyme active site, with its nitrogen in position 3 and the adjacent aniline NH in position 2 establishing a double H-bond with the backbone NH and CO of Cys919, in the enzyme hinge region, respectively; thus corroborating the crucial role of the 2-anilino side moiety.

In conclusion, the ability to exert evident inhibitory effects against VEGFR-2, both in *vitro* and in endothelial cells, together with noteworthy cytotoxicity on HUVECs and *ex vivo* antiangiogenic activity, render the new 2-anilino substituted heteropolycyclic moiety an interesting structure inside the field of VEGFR-2-targeted antitumor agents. Thus, further structural optimization of this promising system is in progress in our laboratories, with the purpose of obtaining new antiangiogenic active candidates.

4. Experimental

4.1. Chemistry

4.1.1. General

The uncorrected melting points were determined using a Reichert Köfler hot-stage apparatus. NMR spectra were obtained on a Bruker AVANCE 400 (^{1}H, 400 MHz, ^{13}C, 100 MHz) in DMSO-d6 (internal standard tetramethylsilane). The coupling constants are given in Hertz. Elemental analyses were performed by our Analytical Laboratory and were within ± 0.4%. Magnesium sulphate was used as the drying agent. Evaporations were made in vacuo (rotating evaporator). Analytical TLC have been carried out on Merck 0.2 mm precoated silica gel aluminium sheets (60 F-254). Silica gel 60 (230-400 mesh) was used

for column chromatography. Combustion analyses on target compounds were performed by our Analytical Laboratory in Pisa. All compounds showed ≥ 95% purity. Reagents, starting materials, and solvents were purchased from commercial suppliers and used as received. According to the methods described previously the following substrates were obtained: 3-Dimethylaminomethylen-2,3-dihydrobenzo[3',2':5,6]thiopyran-4(4*H*)-one **4a**, [22] 7-Methoxy-3-dimethylaminomethylen-2,3-dihydrobenzo[3',2':5,6]thiopyran-4(4*H*)-one **4b** [24], 7-Chloro-3-dimethylaminomethylen-2,3-dihydrobenzo[3',2':5,6]thiopyran-4(4*H*)-one **4c** [20], 4-Substituted-benzamidines hydrochlorides **5b-c** [27,28] and 4-Substituted-benzylguanidines sulphate **6a-c [**29-31].

*4.1.2. General synthetic procedures for 8-substituted-2-amino-5H-benzothiopyrano[4,3-d]pyrimidines **7a-c***

Guanidine hydrochloride (0.160 g, 1.70 mmol) was added, at room temperature, under a nitrogen atmosphere, to a stirred solution of sodium ethoxide (0.059 g, 2.55 mmol of sodium in 8 mL of anhydrous ethanol). The resulting suspension was stirred at room temperature for 15 minutes, then the opportune dimethylaminomethylene derivative **4a-c** (0.85 mmol) was added and the reaction mixture was refluxed for 6 h. After cooling, the resulting suspension was concentrated under reduced pressure and the residue obtained was washed with water and collected to give crude pyrimidines **7a-c**, which were purified by recrystallization from ethanol.

Compound **7a** was already described even if it was obtained with a different synthetic procedure [56]. Compound **7b** was already described by us [20].

*4.1.2.1. 8-Chloro-2-amino-5H-benzothiopyrano[4,3-d]pyrimidine (**7c**).* 75% yield. m. p. 180-182 °C; ^{1}H-NMR (dimethyl-d_6 sulfoxide): δ 3.95 (s, 2H, CH_2S); 6.71 (s, 2H, NH_2 exch.) 7.35-7.41 (dd, 1H, 9-ArH $J_{9\text{-}10}$ = 8.2Hz $J_{9\text{-}7}$ = 2.2 Hz); 7.51 (d, 1H, 7-ArH $J_{7\text{-}9}$ = 2.0 Hz); 8.17 (d, 1H, 10-H $J_{10\text{-}9}$ = 8.0 Hz); 8.24 (s, 1H, 4-ArH)**.** *Anal*. Calcd. for $C_{11}H_8ClN_3S$: C, 52.90; H, 3.21; N, 16.83; Found: C, 52.75; H, 3.24; N, 16.85.

*4.1.3. General synthetic procedures for 8-Substituted-2-(p-substituted-phenyl)-5H-benzothiopyrane[4,3-d]pyrimidines **1a-i***

The appropriate benzamidine hydrochloride **5a-c** (1.70 mmoles) was added, at room temperature, under nitrogen atmosphere, to a stirred solution of sodium ethoxide (0.059 g, 2.55 mmoles of sodium in 8 mL of anhydrous ethanol). The resulting suspension was stirred at room temperature for 15 minutes, then the opportune dimethylaminomethylene derivative **4a-c** (0.187 g, 0.85 mmoles) was added and the reaction mixture was refluxed for 6 hours. After cooling, the suspension was concentrated under reduced pressure. The residue obtained was washed with water and collected, to give crude pyrimidines **1a-i**, which were purified by recrystallization from ethanol.

Compound **1a** was already described [57] even if it was obtained by a different synthetic procedure. Compound **1d** was already described by us [20].

*4.1.3.1. 2-(p-methoxy-phenyl)-5H-benzothiopyrane[4,3-d]pyrimidine (**1b**).* Yield: 30%; M. p. 108-110 °C; ^{1}H NMR (400 Hz, DMSOd_6): δ 3.85 (S, 3H, 4'-OCH_3); 4.16 (s, 2H, CH_2S); 7.10 (d, 2H, 2',6'-ArH, *J* = 8.8 Hz); 7.43-7.49 (m, 3H, 7-, 8-, 9-ArH); 8.45 (dd, 2H, 3',5'-ArH, *J* = 8.6 Hz); 8.52-8.55 (dd, 1H, 10-ArH); 8.81 (s, 1H, 4-ArH). ^{13}C NMR (100 Hz, DMSOd6): δ 26.00, 55.54, 113.52, 114.02, 121.37, 126.01, 128.53, 130.57, 135.61, 136.13, 138.61, 156.41, 161.52. Elemental analysis for $C_{18}H_{14}N_2OS$. Calculated: % C, 70.56; % H, 4.61; % N, 9.14; found % C, 70.17; % H, 4.82; % N, 9.36

*4.1.3.2. 2-(p-chloro-phenyl)-5H-benzothiopyrane[4,3-d]pyrimidine (**1c**).* Yield: 24%; M. p. 114-116 °C; ^{1}H NMR (400 Hz, DMSOd_6): δ 4.20 (s, 2H, CH_2S); 7.42-7.51 (m, 3H, 7-, 8-, 9-ArH); 7.63 (d, 2H, 2',6'-ArH); 8.49-8.56 (m, 3H, 3',5'-, 10-ArH); 8.89 (s, 1H, 4-ArH). ^{13}C NMR (100 Hz, DMSOd_6): δ 26.04, 119.32, 126.14, 127.72, 128.92, 129.34, 132.51,

134.36, 137.04, 156.81, 161.54. Elemental analysis for $C_{17}H_{11}ClN_2S$. Calculated: % C, 65.70; % H, 3.57; % N, 9.01; found % C, 66.02; % H, 3.44; % N, 9.23

*4.1.3.3. 8-Methoxy-2-(p-methoxy-phenyl)-5H-benzothiopyrane[4,3-d]pyrimidine (**1e**).* Yield: 40%; M. p. 186-188 °C; ^{1}H NMR (400 Hz, DMSOd_6): δ 3.85 (S, 6H, 8-OCH_3, 4'-OCH_3); 4.14 (s, 2H, CH_2S); 6.96-7.02 (m, 2H, 7-, 9-ArH); 7.09 (d, 2H, 2',6'-ArH, *J* = 8.6 Hz); 8.41-8.49 (m, 3H, 3',5'-, 10-ArH); 8.73 (s, 1H, 4-ArH). ^{13}C NMR (100 Hz, DMSOd_6): δ 26.25, 54.89, 55.52, 111.32, 111.45, 114.86, 124.18, 126.27, 127.31, 130.36, 138.04, 158.82, 160.85, 162.18. Elemental analysis for $C_{19}H_{16}N_2O_2S$. Calculated: % C, 67.84; % H, 4.79; % N, 8.33; found % C, 67.58; % H, 4.59; % N, 8.21

*4.1.3.4. 8-Methoxy-2-(p-chloro-phenyl)-5H-benzothiopyrane[4,3-d]pyrimidine (**1f**).* Yield: 35%; M. p. 142-144 °C; ^{1}H NMR (400 Hz, DMSOd_6): δ 3.86 (S, 3H, 8-OCH_3); 4.17 (s, 2H, CH_2S); 6.96-7.03 (m, 2H, 7-, 9-ArH); 7.61 (d, 2H, 2',6'-ArH); 8.46-8.51 (m, 3H, 3',5'-, 10-ArH); 8.79 (s, 1H, 4-ArH). ^{13}C NMR (100 Hz, DMSOd_6): δ 26.24, 55.60, 112.01, 113.33, 121.31, 124.37, 128.70, 129.03, 129.36, 135.53, 136.04, 138.45, 155.40, 157.41, 161.12, 161.70. Elemental analysis for $C_{18}H_{13}ClN_2OS$. Calculated: % C, 63.43; % H, 3.84; % N, 8.22; found % C, 63.25; % H, 3.63; % N, 7.99

*4.1.3.5. 8-Chloro-2-phenyl-5H-benzothiopyrane[4,3-d]pyrimidine (**1g**).* Yield: 14%; M. p. 117-119 °C; ^{1}H NMR (400 Hz, DMSOd_6): δ 4.22 (s, 2H, CH_2S); 7.46-7.51 (dd, 1H, 9-ArH $J_{9\text{-}10}$ = 8.6 Hz, $J_{9\text{-}7}$ = 2.2 Hz); 7.54-7.57 (m, 3H, 2'-, 4'-, 6'-ArH); 7.62 (d, 1H, 7-ArH, *J* = 2.0 Hz); 8.47-8.57 (m, 3H, 3'-, 5'-, 10-ArH); 8.88 (s, 1H, 4-ArH). ^{13}C NMR (100 Hz, DMSOd_6): δ 26.22, 117.18, 125.72, 126.18, 127.54, 128.58, 129.21, 131.19, 135.10,

158.78, 161.19. Elemental analysis for $C_{17}H_{11}ClN_2S$. Calculated: % C, 65.70; % H, 3.57; % N, 9.01; found % C, 65.59; % H, 3.67; % N, 8.89

*4.1.3.6. 8-Chloro-2-(p-methoxy-phenyl)-5H-benzothiopyrane[4,3-d]pyrimidine (**1h**).* Yield: 13%; M. p. 142-144 °C; ^{1}H NMR (400 Hz, DMSOd_6): δ 3.86 (S, 3H, 8-OCH_3); 4.21 (s, 2H, CH_2S); 7.11 (d, 2H, 2',6'-ArH, *J* = 8.8 Hz); 7.47-7.52 (dd, 1H, 9-ArH, $J_{9\text{-}10}$ = 8.6 Hz, $J_{9\text{-}7}$ = 2.2 Hz); 7.63 (d, 1H, 7-ArH, *J* = 2.2 Hz); 8.45 (d, 2H, 3',5'-ArH, *J* = 8.8 Hz); 8.53 (d, 1H, 10-ArH, *J* = 8.4 Hz); 8.90 (s, 1H, 4-ArH). ^{13}C NMR (100 Hz, DMSOd_6): δ 26.23, 55.58, 114.83, 117.21, 125.63, 126.15, 128.56, 130.31, 133.46, 138.47, 158.81, 160.64, 162.21. Elemental analysis for $C_{18}H_{13}ClN_2OS$. Calculated: % C, 63.43; % H, 3.84; % N, 8.22; found % C, 63.33; % H, 3.64; % N, 7.87

*4.1.3.7. 8-Chloro-2-(p-chloro-phenyl)-5H-benzothiopyrane[4,3-d]pyrimidine (**1i**).* Yield: 15%; M. p. 165-167 °C; ^{1}H NMR (400 Hz, DMSOd_6): δ 4.24 (s, 2H, CH_2S); 7.46-7.52 (dd, 1H, 9-ArH $J_{9\text{-}10}$ = 8.4 Hz, $J_{9\text{-}7}$ = 2.0 Hz); 7.61-7.65 (m, 3H, 2',6'-, 7-ArH); 8.49 (m, 3H, 3',5'-, 10-ArH); 8.90 (s, 1H, 4-ArH). ^{13}C NMR (100 Hz, DMSOd_6): δ 26.23, 122.31, 126.54, 127.15, 128.77, 128.90, 129.42, 130.46, 135.74, 135.75, 136.26, 138.78, 156.14, 156.64, 161.34. Elemental analysis for $C_{17}H_{10}Cl_2N_2S$. Calculated: % C, 59.14; % H, 2.92; % N, 8.11; found % C, 59.36; % H, 3.12; % N, 7.94

*4.1.4. General synthetic procedures for 8-Substituted-2-(p-substituted-anilino)-5H-benzothiopyrane[4,3-d]pyrimidines **2a-i***

The opportune 8-substituted-2-amino-5*H*-benzothiopyrane[4,3-*d*]pyrimidine **7a-c** (0.417 mmoles) was added, at room temperature, under nitrogen atmosphere, to 0.079 g of CuI (0.417 mmoles) and 0.115 g of anhydrous K_2CO_3 (0.833 mmoles). Then, the appropriate

aryl iodide (0.694 mmoles) and 0.04 mL of DMEDA (0.417 mmoles) and 2.5 mL of dioxane were added. The reaction mixture was heated at 100 °C and allowed to stir for 24 hours. After cooling, the mixture was supplemented with 2.5 mL of concentrated NH_3 aqueous solution and 10-15 mL of a saturated solution of NaCl. The reaction mixture was extracted with ethylacetate and the organic layers obtained were evaporated under reduced pressure giving a residue. This latter was purified by flash chromatography using petroleum ether 60-80 °C/ethyl acetate 70:30 as the eluting system, to yield compounds **2a-i**.

Compound **2a** has been already described [41], even it was obtained by a different synthetic pathway.

*4.1.4.1. 2-anilino-5H-benzothiopyrane[4,3-d]pyrimidine (**2a**).* Yield: 22 %; M. p. 161-162 °C; ^{1}H NMR (400 Hz, DMSOd_6): δ 4.02 (s, 2H, CH_2S); 6.97 (t, 1H, 4'-ArH); 7.31 (t, 2H, 8,9-ArH); 7.38-7.43 (m, 3H, 7, 3',5'-ArH); 7.81 (d, 2H, 2',6'-ArH *J* = 7,6 Hz); 8.29 (d, 1H, 10-ArH *J* = 7,2 Hz); 8.46 (s, 1H, 4-ArH); 9.68(s, 1H, NH exch.). ^{13}C NMR (100 Hz, DMSOd_6): δ 25.92, 115.11, 118.67, 121.27, 126.22, 127.02, 127.90, 128.50, 131.14, 132.09, 136.52, 140.55, 156.39, 157.73, 159.36. Elemental analysis for $C_{17}H_{13}N_3S$. Calculated: % C, 70.08; % H, 4.50; % N, 14.42; found % C, 69.93; % H, 4.56; % N, 14.36

*4.1.4.2. 2-(p-methoxy-anilino)-5H-benzothiopyrane[4,3-d]pyrimidine (**2b**).* Yield: 16%; M. p. 164-165 °C; ^{1}H NMR (400 Hz, DMSOd_6): δ 3.74 (S, 3H, 8-OCH_3); 4.00 (s, 2H, CH_2S); 6.91 (d, 2H, 2',6'-ArH *J* = 9,0 Hz); 7.35-7.44 (m, 3H, 7-, 8-, 9-ArH); 7.69 (d, 2H, 3',5'-ArH *J* = 9.0 Hz); 8.26-8.29 (dd, 1H, 10-ArH); 8.42 (s, 1H, 4-ArH); 9.47 (s, 1H, NH exch.). ^{13}C NMR (100 Hz, DMSOd_6): δ 25.91. 55.57, 115,17, 118.76, 119.14, 121.76, 125.63, 127.81,

128.64, 131.24, 132.56, 137.03, 159.91, 163.24. Elemental analysis for $C_{18}H_{15}N_3OS$. Calculated: % C, 67.27; % H, 4.70; % N, 13.07; found % C, 67.43; % H, 4.56; % N, 12.96

*4.1.4.3. 2-(p-chloro-anilino)-5H-benzothiopyrane[4,3-d]pyrimidine (**2c**).* Yield: 23%; M. p. 226-228 °C; ^{1}H NMR (400 Hz, DMSOd_6): δ 4.03 (s, 2H, CH_2S); 7.34-7.45 (m, 5H, 3'-, 5'-, 7-, 8-, 9-ArH); 7.85 (d, 2H, 2',6'-ArH *J* = 9.0 Hz); 8.29 (d, 1H, 10-ArH); 8.49 (s, 1H, 4-ArH); 9.86 (s, 1H, NH exch.). ^{13}C NMR (100 Hz, DMSOd_6): δ 25.93, 118.61, 119.27, 122.34, 125.71, 127.72, 128.61, 129.67, 132.51, 137.04, 159.91, 163.42. Elemental analysis for $C_{17}H_{12}ClN_3S$. Calculated: %C, 62.67; % H, 3.71; % N, 12.90; found % C, 62.84; % H, 3.58; % N, 13.11

*4.1.4.4. 8-Methoxy-2-anilino-5H-benzothiopyrane[4,3-d]pyrimidine (**2d**).* Yield: 13%; M. p. 174-176 °C; ^{1}H NMR (400 Hz, DMSOd_6): δ 3.83 (S, 3H, 8-OCH_3); 4.01 (s, 2H, CH_2S); 6.91-6.99 (m, 3H, 7-, 9-, 4'-ArH); 7.30 (t, 2H, 3',5'-ArH); 7.81 (d, 2H, 2',6'-ArH); 8.24 (d, 1H, 10-ArH); 8.40 (s, 1H, 4-ArH); 9.61 (s, 1H, NH exch.). ^{13}C NMR (100 Hz, DMSOd_6): δ 26.19, 111.27, 117.83, 118.61, 122.48, 124.13, 129.52, 159.91, 160.82, 164.82, 164.38, 167.21. Elemental analysis for $C_{18}H_{15}N_3OS$. Calculated: %C, 67.27; % H, 4.70; % N, 13.07; found % C, 66.96; % H, 4.87; % N, 13.24

*4.1.4.5. 8-Methoxy-2-(p-methoxy-anilino)-5H-benzothiopyrane[4,3-d]pyrimidine (**2e**).* Yield: 12%; M. p. 195-197 °C; ^{1}H NMR (400 Hz, DMSOd_6): δ 3.74 (S, 3H, 4'-OCH_3); 3.83 (S, 3H, 8-OCH_3); 4.00 (s, 2H, CH_2S); 6.88-6.98 (m, 4H, 2',6'-, 7-, 9-ArH); 7.69 (d, 2H, 3',5'-ArH, *J* = 9.0 Hz); 8.22 (d, 1H, 10-ArH, *J* = 9.0 Hz); 8.35 (s, 1H, 4-ArH); 9.40 (s, 1H, NH exch.). ^{13}C NMR (100 Hz, DMSOd_6): δ 26.21, 54.92, 55.56, 111.34, 112.05,

115.17, 118.62, 121.73, 124.16, 131.22, 138.09, 153.36, 159.97, 160.82, 164.82. Elemental analysis for $C_{19}H_{17}N_3O_2S$. Calculated: % C, 64.94; % H, 4.88; % N, 11.96; found % C, 65.22; % H, 5.09; % N, 12.11

*4.1.4.6. 8-Methoxy-2-(p-chloro-anilino)-5H-benzothiopyrane[4,3-d]pyrimidine (**2f**).* Yield: 35%; M. p. 214-216 °C; ^{1}H NMR (400 Hz, DMSOd_6): δ 3.83 (S, 3H, OCH_3); 4.02 (s, 2H, CH_2S); 6.94-6.99 (dd, 2H, 7-, 9-ArH); 7.35 (d, 2H, 3',5'-ArH, *J* = 9.0 Hz); 7.84 (d, 2H, 2',6'-ArH, *J* = 8.8 Hz); 8.23 (d, 1H, 10-ArH, *J* = 8.2 Hz); 8.42 (s, 1H, 4-ArH); 9.79 (s, 1H, NH exch.). ^{13}C NMR (100 Hz, DMSOd_6): δ 26.13, 55.54, 112.16, 112.98, 114.31, 119.99, 124.52, 124.67, 128.30, 128.76, 138.48, 139.66, 155.87, 157.82, 159.01, 161.32. Elemental analysis for $C_{18}H_{14}ClN_3OS$. Calculated: % C, 60.76; % H, 3.97; % N, 11.81; found % C, 60.52; % H, 3.78; % N, 11.73

*4.1.4.7. 8-Chloro-2-anilino-5H-benzothiopyrane[4,3-d]pyrimidine (**2g**).* Yield: 70%; M. p. 222-224 °C; ^{1}H NMR (400 Hz, DMSOd_6): δ 4.06 (s, 2H, CH_2S); 6.97 (t, 1H, 4'-ArH); 7.36 (t, 2H, 3',5'-ArH);7.44-7.49(dd, 1H, 9-ArH $J_{9\text{-}10}$ = 8.6 Hz, $J_{9\text{-}7}$ = 2.2 Hz); 7.57 (d, 1H, 7-ArH); 7.80 (d, 2H, 2',6'-ArH); 8.27 (d, 1H, 10-ArH *J* = 8.6 Hz); 8.49 (s, 1H, 4-ArH); 9.73 (s, 1H, NH exch.). ^{13}C NMR (100 Hz, DMSOd_6): δ 25.90, 114.71, 118.75, 121.37, 127.13, 128.49, 128.53, 130.90, 135.69, 138.85, 140.43, 156.61, 156.91, 159.36. Elemental analysis for $C_{17}H_{12}ClN_3S$. Calculated: % C, 62.67; % H, 3.71; % N, 12.90; found % C, 62.41; % H, 3.44; % N, 13.11

*4.1.4.8. 8-Chloro-2-(p-methoxy-anilino)-5H-benzothiopyrane[4,3-d]pyrimidine (**2h**).* Yield: 10%; M. p. 205-207 °C; ^{1}H NMR (400 Hz, DMSOd6): δ 3.74 (S, 3H, 4'-OCH_3); 4.05 (s, 2H, CH_2S); 6.91 (d, 2H, 3',5'-ArH, *J* = 9.0 Hz); 7.43-7.48 (dd, 1H, 9-ArH); 7.56 (d,

1H, 7-ArH); 7.67 (d, 2H, 2',6'-ArH, *J* = 8.8 Hz); 8.25 (d, 1H, 10-ArH); 8.44 (s, 1H, 4-ArH); 9.52 (s, 1H, NH exch.). ^{13}C NMR (100 Hz, DMSOd$_6$): δ 25.92, 55.14, 113.74, 114.10, 120.55, 126.25, 127.10, 128.50, 130.97, 133.54, 135.58, 138.80, 154.21, 156.59, 156.83, 159.53. Elemental analysis for $C_{18}H_{14}ClN_3OS$. Calculated: % C, 60.76; % H, 3.97; % N, 11.81; found %C, 60.96; %H, 3.66; % N, 12.17

*4.1.4.9. 8-Chloro-2-(p-chloro-anilino)-5H-benzothiopyrane[4,3-d]pyrimidine (**2i**)* Yield: 12%; M. p. 170-172 °C; ^{1}H NMR (400 Hz, DMSOd$_6$): δ 4.06 (s, 2H, CH_2S); 7.36 (d, 2H, 3',5'-ArH, *J* = 8.8 Hz); 7.41-7.47 (dd, 1H, 9-ArH $J_{9\text{-}10}$ = 8.6 Hz, $J_{9\text{-}7}$ = 2.2 Hz); 7.57 (d, 1H, 7-ArH, *J* = 2.2 Hz); 7.83 (d, 2H, 2',6'-ArH, *J* = 9.0 Hz); 8.26 (d, 1H, 10-ArH, *J* = 8.6 Hz); 8.50 (s, 1H, 4-ArH); 9.89 (s, 1H, NH exch.). ^{13}C NMR (100 Hz, DMSOd$_6$): δ 25.89, 115.12, 120.15, 124.78, 126.35, 127.16, 128.36, 128.63, 130.79, 131.54, 135.78, 138.92, 139.45, 156.63, 159.11. Elemental analysis for $C_{17}H_{11}Cl_2N_3S$. Calculated: % C, 56.20; % H, 3.88; % N, 11.57; found % C, 55.94; % H, 3.59; % N, 11.83

*4.1.5. General synthetic procedures for 8-Substituted-2-(p-substituted-Benzylamino)-5H-benzothiopyrano[4,3-d]pyrimidines **3a-i***

The appropriate benzylguanidine sulfate **6a-c** (1.70 mmoles) was added, at room temperature, under nitrogen atmosphere, to a stirred solution of sodium ethoxide (0.059 g, 2.55 mmoles of sodium in 8 mL of anhydrous ethanol). The resulting suspension was stirred at room temperature for 15 minutes, then the appropriate dimethylaminomethylene derivative **1a-c** (0.187 g, 0.85 mmoles) was added, and the reaction mixture was refluxed for 6 hours. After cooling, the suspension was concentrated under reduced pressure. The residue obtained was washed with water and collected, to give crude pyrimidines **3a-i**, which were purified by recrystallization from ethanol.

*4.1.5.1. 2-Benzylamino-5H-benzothiopyrano[4,3-d]pyrimidine (**3a**).* Yield: 20%; M. p. 144-146 °C; ^{1}H NMR (400 Hz, DMSOd_6): δ 3.92 (s, 2H, CH_2S); 4.56 (d, 2H, $\underline{CH_2}NH$, *J* = 6.4 Hz) 7.16-7.39 (m, 8H, 7-, 8-, 9-, 2'-, 3'-, 4'-, 5', 6'-ArH) 7.81 (t, 1H, $CH_2\underline{NH}$ exch. *J* = 6.3 Hz); 8.19 (d, 1H, 10-ArH, *J* = 7.6 Hz); 8.26 (s, 1H, 4-ArH). ^{13}C NMR (400 Hz, DMSOd_6): δ 25.93, 44.18, 126.00, 126.47, 126.89, 127.11, 127.74, 128.24, 130.82, 140.59, 161.80. Elemental analysis for $C_{18}H_{15}N_3S$. Calculated: % C, 70.79; % H, 4.95; % N, 13.76; found % C, 70.52; % H, 4.77; % N, 13.99

*4.1.5.2. 2-(p-Methoxy-benzylamino-5H-benzothiopyrano[4,3-d]pyrimidine (**3b**).* Yield: 25%; M. p. 160-162 °C; ^{1}H NMR (400 Hz, DMSOd_6): δ 3.70 (S, 3H, -OCH_3); 3.92 (s, 2H, CH_2S); 4.48 (d, 2H, $\underline{CH_2}NH$, *J* = 6.2 Hz) 6.85-(d, 2H, 2',6'-ArH, *J* = 8.4 Hz); 7.26-7.39 (m, 5H, 7-, 8-, 9-, 3',5'-ArH); 7.71 (t, 1H, $CH_2\underline{NH}$ exch., *J* = 6.3 Hz); 8.20-8.25 (m, 2H, 10-, 4-ArH). ^{13}C NMR (100 Hz, DMSOd_6): δ 25.88, 43.57, 54.94, 113.52, 125.97, 126.86, 127.70, 128.39, 130.76, 132.43, 157.98, 161.73. Elemental analysis for $C_{19}H_{17}N_3OS$. Calculated: % C, 68.03; % H, 5.11; % N, 12.53; found % C, 67.78; % H, 5.32; % N, 12.67

*4.1.5.3. 2-(p-Chloro-benzylamino-5H-benzothiopyrano[4,3-d]pyrimidine (**3c**).* Yield: 31%; M. p. 152-154 °C; ^{1}H NMR (400 Hz, DMSOd_6): δ 3.92 (s, 2H, CH_2S); 4.53 (d, 2H, $\underline{CH_2}NH$, *J* = 6.0 Hz); 7.28-7.39 (m, 7H, 7-, 8-, 9-, 2',6'-, 3',5'-ArH); 7.82 (t, 1H, $CH_2\underline{NH}$ exch., *J* = 5.9 Hz); 8.17 (d, 1H, 10-ArH, *J* = 7.2 Hz); 8.26 (s, 1H, 4-ArH). ^{13}C NMR (100 Hz, DMSOd_6): δ 25.90, 43.62, 126.02, 126.89, 127.75, 128.09, 128.09, 130.86, 139.69. Elemental analysis for $C_{18}H_{14}ClN_3S$. Calculated: % C, 63.62; % H, 4.15; % N, 12.36; found % C, 63.39; % H, 4.27; % N, 12.07

*4.1.5.4. 8-Methoxy-2-benzylamino-5H-benzothiopyrano[4,3-d]pyrimidine (**3d**).* Yield: 12%; M. p. 167-169 °C; ^{1}H NMR (400 Hz, DMSOd$_6$): δ 3.80 (S, 3H, 8-OCH$_3$); 3.91 (s, 2H, CH$_2$S); 4.54 (d, 2H, CH$_2$NH, *J* = 6.4 Hz); 6.87-6.92 (m, 2H, 7-, 9-ArH); 7.19-7.33 (m, 5H, 2'-, 3'-, 4'-, 5', 6'-ArH); 7.72 (t, 1H, CH$_2$NH exch. *J* = 6.3 Hz); 8.13 (d, 1H, 10-ArH, *J* = 8.8 Hz); 8.19 (s, 1H, 4-ArH). ^{13}C NMR (100 Hz, DMSOd$_6$): δ 26.18, 44.17, 55.48, 111.98, 112.73, 126.43, 127.09, 128.12, 140.67. Elemental analysis for $C_{19}H_{17}N_3OS$. Calculated: % C, 68.03; % H, 5.11; % N, 12.53; found % C, 67.96; % H, 5.18; % N, 12.61

*4.1.5.5. 8-Methoxy-2-(p-methoxy-benzylamino)-5H-benzothiopyrano[4,3-d]pyrimidine (**3e**).* Yield: 25%; M. p. 140-142 °C; ^{1}H NMR (400 Hz, DMSOd$_6$): δ 3.70 (S, 3H, 4'-OCH$_3$); 3.80 (S, 3H, 8-OCH$_3$); 3.90 (s, 2H, CH$_2$S); 4.46 (d, 2H, CH$_2$NH, *J* = 6.0 Hz) 6.85-(d, 2H, 2',6'-ArH, *J* = 8.4 Hz); 6.90 (d, 1H, 9-ArH, *J* = 9.8); 6.92 (s, 1H, 7-ArH); 7.27 (d, 2H, 3',5'-ArH, *J* = 8.4 Hz); 7.62 (t, 1H, CH$_2$NH exch., *J* = 6.0 Hz); 8.15 (d, 1H, 10-ArH, *J* = 9.8 Hz); 8.18 (s, 1H, 4-ArH). ^{13}C NMR (100 Hz, DMSOd$_6$): δ 26.18, 43.89, 54.93, 55.58, 111.23, 111.35, 112.08, 114.17, 118.67, 124.18, 130.51, 132.23, 138.05, 158.61, 159.73, 159.92, 160.83, 164.41. Elemental analysis for $C_{20}H_{19}N_3O_2S$. Calculated: % C, 64.94; % H, 4.88; % N, 11.96; found % C, 65.19; % H, 4.69; % N, 12.27

*4.1.5.6. 8-Methoxy-2-(p-chloro-benzylamino)-5H-benzothiopyrano[4,3-d]pyrimidine (**3f**).* Yield: 29%; M. p. 170-172 °C; ^{1}H NMR (400 Hz, DMSOd$_6$): δ 3.80 (S, 3H, OCH$_3$); 3.91 (s, 2H, CH$_2$S); 4.52 (d, 2H, CH$_2$NH, *J* = 6.4 Hz); 6.85-6.93 (m, 2H, 7-, 9-ArH); 7.36-7.42 (m, 4H, 2',6'-, 3',5'-ArH); 7.74 (t, 1H, CH$_2$NH exch., *J* = 6.3 Hz); 8.11 (d, 1H, 10-ArH); 8.19 (s, 1H, 4-ArH). ^{13}C NMR (100 Hz, DMSOd$_6$): δ 26.11, 43.60, 55.50, 112.00, 112.76,

128.07, 128.53, 128.94, 130.93, 161.05. Elemental analysis for $C_{19}H_{16}ClN_3OS$. Calculated: % C, 61.70; % H, 4.36; % N, 11.36; found % C, 61.99; % H, 4.17; % N, 10.98

*4.1.5.7. 8-Chloro-2-benzylamino-5H-benzothiopyrano[4,3-d]pyrimidine (**3g**).* Yield: 14%; M. p. 158-160 °C; ^{1}H NMR (400 Hz, DMSOd_6): δ 3.96 (s, 2H, CH_2S); 4.55 (d, 2H, $\underline{CH_2}NH$, *J* = 6.2 Hz) 7.19-7.39 (m, 6H, 9-, 2'-, 3'-, 4'-, 5', 6'-ArH); 7.51 (d, 1H, 7-ArH, *J* = 1.8 Hz); 7.86 (t, 1H, $CH_2\underline{NH}$ exch. *J* = 6.4 Hz); 8.17 (d, 1H, 10-ArH); 8.27 (s, 1H, 4-ArH). ^{13}C NMR (100 Hz, DMSOd_6): δ 25.89, 44.17, 126.07, 126.48, 126.95, 127.10, 128.12, 128.40, 135.35, 140.46, 161.77. Elemental analysis for $C_{18}H_{14}ClN_3S$. Calculated: % C, 63.62; % H, 4.15; % N, 12.36; found % C, 63.89; % H, 3.99; % N, 12.22

*4.1.5.8. 8-Chloro-2-(p-methoxy-benzylamino)-5H-benzothiopyrano[4,3-d]pyrimidine (**3h**).* Yield: 13%; M. p. 165-167 °C; ^{1}H NMR (400 Hz, DMSOd_6): δ 3.33 (S, 3H, 4'-OCH_3); 3.95 (s, 2H, CH_2S); 4.48 (d, 2H, $\underline{CH_2}NH$, *J* = 6.2 Hz) 6.86 (d, 2H, 2',6'-ArH, *J* = 8.8 Hz); 7.28 (d, 2H, 3',5'-ArH, *J* = 9.0 Hz); 7.37-7.42 (dd, 1H, 9-ArH, $J_{9\text{-}10}$ = 8.9 Hz, $J_{9\text{-}7}$ = 2.0 Hz); 7.51 (d, 1H, 7-ArH, $J_{9\text{-}7}$ = 2.0 Hz); 7.76 (t, 1H, $CH_2\underline{NH}$ exch. *J* = 6.2 Hz); 8.21 (d, 1H, 10-ArH, *J* = 8.9 Hz); 8.27 (s, 1H, 4-ArH). ^{13}C NMR (100 Hz, DMSOd_6): δ 26.22, 43.94, 55.56, 114.18, 117.17, 118.64, 125.71, 128.52, 129.13, 130.53, 132.24, 133.46, 159.72, 159.91, 164.43. Elemental analysis for $C_{19}H_{16}ClN_3OS$. Calculated: % C, 61.70; % H, 4.36; % N, 11.36; found % C, 62.09; % H, 4.17; % N, 11.61

*4.1.5.9. 8-Chloro-2-(p-chloro-benzylamino)-5H-benzothiopyrano[4,3-d]pyrimidines (**3i**).* Yield: 12%; M. p. 185-187 °C; ^{1}H NMR (400 Hz, DMSOd_6): δ 3.97 (s, 2H, CH_2S); 4.54 (d, 2H, $\underline{CH_2}NH$, *J* = 6.4 Hz) 7.34-7.40 (m, 5H, 2',6'-, 3',5'-, 9-ArH); 7.51 (d, 1H, 7-H, *J* = 2.2 Hz); 7.87 (t, 1H, $CH_2\underline{NH}$ exch. *J* = 6.4 Hz); 8.17 (d, 1H, 10-ArH, *J* = 8.8 Hz); 8.28 (s,

1H, 4-ArH). ^{13}C NMR (100 Hz, DMSOd_6): δ 26.23, 43.92, 117.15, 118.61, 125.72, 128.63, 129.34, 132.37, 133.45, 138.02, 138.47, 159.71, 159.93, 164.42. Elemental analysis for $C_{18}H_{13}Cl_2N_3S$. Calculated: % C, 57.76; % H, 3.50; % N, 11.23; found % C, 58.04; % H, 3.71; % N, 10.97

4.2. Biological evaluation

4.2.1. In vitro assay for VEGFR-2 activity

The VEGFR-2 kinase assay has been performed by using the recombinant human enzyme (Life technologies) and the fluorescence peptide substrate-based assay Omnia Tyr Peptide 8 (Invitrogen). Briefly, 15 μL of reaction mixture containing kinase reaction buffer, 1 mM ATP, 0.2 mM DTT and Omnia Peptide Substrate as indicated by the manufacturer was incubated at 30 °C for 5 min in 96-well microtiter plates. After addition of VEGFR-2 the samples (final volume of 20 μL) were incubated for further 50 min in the absence (control) or in the presence of different concentrations of test compounds and during incubation the fluorescence intensity (λ_{ex} = 355 nm, λ_{em} = 460 nm) was recorded on a Victor 1460 Multilabel counter (Perkin Elmer).

4.2.2. Inhibition growth assay

HeLa (human cervix adenocarcinoma cells) and A-431 (skin carcinoma squamous cells) were grown in Nutrient Mixture F-12 [HAM] (Sigma Chemical Co.) and Dulbecco's modified Eagle's medium (Sigma Chemical Co.) respectively, supplemented with 10% heat-inactivated fetal calf serum (Invitrogen). MSTO-211H (human biphasic mesothelioma cells) were grown in RPMI 1640 (Sigma Chemical Co.) supplemented with 2.4 g/L Hepes, 0.11 g/L Na-pyruvate and 10% heat-inactivated fetal calf serum (Invitrogen). 100 U/mL

penicillin, 100 μg/mL streptomycin and 0.25 μg/mL amphotericin B (Sigma Chemical Co.) were added to the media. HUVECs (human umbilical vein endothelian cells) were purchased from Lonza Ltd. and maintained as recommended. The cells were cultured at 37 °C in a moist atmosphere of 5% carbon dioxide in air.

Cells ($3\text{-}4x10^4$) were seeded into each well of a 24-well cell culture plate. After incubation for 24 h, various concentrations of the test agents were added. The cells were then incubated in standard conditions for a further 72 h.

A trypan blue assay was performed to determine cell viability. Cytotoxicity data were expressed as GI_{50} values, i.e., the concentration of the test agent inducing 50% reduction in cell number compared with control cultures.

4.2.3. Phospho-VEGFR-2 inhibition assay

HUVECs ($2x10^5$ cells/well) were seeded and maintained in 1% FBS medium. After 24 h, cells were treated for 72 h with **2b**, **2e** and **2i** at a concentration corresponding to the experimental GI_{50} of cell proliferation, at a higher concentration (2.5 μM) and at a lower concentration (0.1 μM), or with vehicle alone. The DMSO concentration in control's media was the one used to dilute the highest concentration of the compound in the same experiment. The media were supplemented with rhVEGF (10 ng/mL). At the end of the experiment, the media was removed, the cells were rinsed with ice-cold PBS and directly lysed with 0.5 mL of ice-cold 1X lysis buffer (20 mM Tris pH7.5, 150 mM, 1 mM EDTA, 1 mM EGTA, 1% triton X-100, 2.5 mM sodium pyrophosphate, 1 mM β-glycerolphosphate, 1mM Na_3VO_4, 1 μg/mL leupetin; Cell Signaling Technology, MA, USA, cat.#9803) and 1 mM PMSF to each plate for 5 min at 4 °C. Lysates were collected and sonicated on ice for 10 s. The samples were microcentrifuged for 10 min at 4 °C and the supernatant was collected. Endothelial cell lysates were assayed as *per* the

manufacturer's instructions with PathScan phospo-VEGFR-2 (Tyr1175) and with the Total VEGFR-2 sandwich ELISA kits (Cell Signaling Technology). The optical density was determined using a Multiskan Spectrum microplate reader (Thermo Labsystems, Milan, Italy) set to 450 nm. All experiments were repeated, independently, three times with at least 9 samples for each drug concentration.

4.2.4. Ex vivo "rat aortic ring" assay

The assay was performed with some modifications of the method originally reported by Nicosia and Ottinetti.[35] The artery was dissected from the aortic arch to the diaphragm, and the periaortic fibroadipose tissue was carefully removed keeping it in a Petri dish with nutrient Krebs solution (NaCl 118 mM, KCl 4.7 mM, $CaCl_2$ 1.8 mM, KH_2PO_4 1.2 mM, $NaHCO_3$ 25.0 mM, glucose 11.0 mM). One-millimetre length aortic rings were sectioned, transferred to a small Petri plate containing Endothelial cell basal medium MV2, (EBM MV2, Promocell, Heidelberg, Germany), and antibiotics (gentamicin 30µg/mL, amphotericin 0.015µg/mL), to avoid possible contamination. The assay was performed in a 96-well flat-bottomed plate, which was kept on ice until use. All the materials that come in contact with Matrigel would be cold in order to prevent its solidification, which takes place at room temperature. Likewise, Matrigel was kept on ice in cold chamber (4 °C), for at least 4 hours before the experiment took place. 50 µL of Matrigel per well were added, and the aortic rings were randomized into wells. After 15 minutes at room temperature Matrigel polymerized, and 200 µL of EBM MV2 growth medium, preheated to 37 °C, were added. Finally 20 µL of the drug, whose effect is intended to be studied, were added to the appropriate wells. The plate was incubated at 37 °C and 5% CO_2 for 7 days, renewing the medium, as well as the stimuli required the day after starting the experiment, and every two days.

4.2.5. Image acquisition

To daily monitoring the new vessels growth, cultures were daily photographed (days 3–7) on an inverted microscope Leica DM IL LED with a Leica Camera (objective 2.5x) and analyzed by Leica Microsystems LAS Software V3.7.0 (Heerbrugg Switzerland). To determine the growth kinetic, it was measured in microns the distance in the *x* and *y* axis, taking as point source, in each case, the outer surface of the ring (Figure 6A). The mean of *x* and *y* values indicate the angiogenic growth for each aortic explant. In addition, on the 7th day, a final time fluorescence cell staining was also performed. For this purpose, 1µL of calcein (Molecular Probes Inc. InvitrogenTM Paisley, UK) was added, and after incubating for 15 minutes, the images were visualized using a Nikon fluorescence microscope Eclipse E800 equipped with Nikon camera, (4x objective) and captured using the software Nikon ACT-1 (Figure 6B).

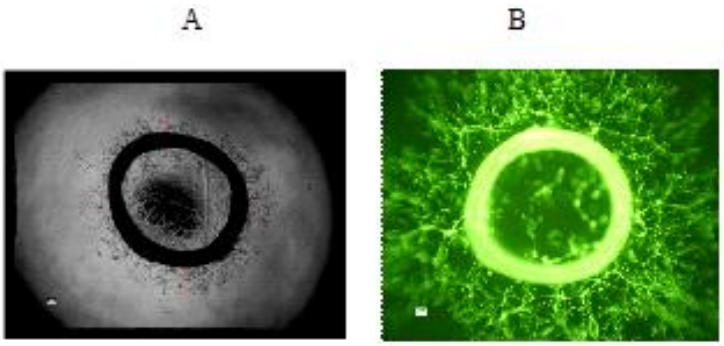

Figure 6. Visualization of the angiogenic growth: (A) at day 3 (Leica DM IL LED Leica camera, 2.5x objective). (B) Fluorescence cell staining at day 7 (Nikon fluorescence microscope Eclipse E800 equipped with Nikon camera, 4x objective).

4.2.6. In vitro EGFR Inhibition Assay

The inhibitory activity of the test compounds was assayed by adding 5 µL of the inhibitor solution to the reaction mixture described above. All the products were dissolved in 100% DMSO and diluted to the appropriate concentrations with Tyrosine Kinase Reaction Buffer, provided by the kit. Final concentration of DMSO in assays solutions never exceed 1%,, and proved to have no effects on protein activity. Determination of the IC_{50} values was performed by linear regression analysis of the log-dose response curve, which was generated using at least five concentrations, between 100 µM and 10 nM, of the inhibitor causing an inhibition between 20% and 80%, with two replicates at each concentration. Gefitinib (IC_{50} = 0.022 µM) was exploited as the reference standard. The 95% confidence limits (95% CL) were calculated from *t* values for *n* - 2, where *n* is the total number of determinations (Table 3). Tests were performed at 30 °C in 96-well microtiter plates, exploiting the Omnia Tyr Peptide 7 Kit (Invitrogen). Briefly, 5 µL of 3 mU/µL EGFR was added to a reaction mixture containing 5 µL of Tyrosine Kinase, Reaction Buffer, 5 µL of Tyrosine Kinase Substrate, 5 µL of 1 mM ATP, 5µL of 1 mM DTT, 25 µL of ultrapure water and the reaction was monitored with the fluorescence meter Victor3™ PerkinElmer at 360 nm (excitation) and 485 nm (emission). Kinase activity of the target protein was calculated from a linear least-squares fit of the data for fluorescence intensity versus time.

4.2.7. In vitro Kinases Enzymatic Inhibition

The screening of compounds **1d**, **2b** and **2i** on a set of 10 human kinases (Akt1/PKBα, AurA/Aur2 kinase, CDC2/CDK1, ERK1, FAK, MEK1/MAP2K1, PDGFRβ kinase, RAF-1 kinase, ROCK1, Src kinase) was performed by CEREP (France),

according to the company's standard operating procedures, (Figures 4a-c, Tables S1a,b).

4.3. Molecular Modelling

The new version of the docking program AutoDock (version 4.2, AD4) [69,70], as implemented through the graphical user interface called AutoDockTools (ADT), was used to perform cross-docking experiments on the VEGFR-2 X-ray structures having PDB codes: 1YWN, 2P2H, 2XIR, 3BE2, 3EWH, 3VHE, 3VNT, 3VO3, 4AG8, 4ASE. These structure were prepared using the Protein Preparation Wizard in Maestro (Protein Preparation Wizard, Schrödinger, LLC, New York, NY), which assigns bond orders, adds hydrogen atoms, deletes water molecules, and generates appropriate protonation states. Maestro was also used to superimpose all the complexes on the 1YWN structure.

The ligand and the receptor structures were then converted to AD4 format files using ADT generating automatically all other atom values. The docking area was centered on the putative binding site. A set of grids of 60 Å × 60 Å × 60 Å with 0.375 Å spacing was calculated around the docking area for the ligand atom types using AutoGrid4. For each ligand, 200 separate docking calculations were performed. Each docking calculation consisted of 10 million energy evaluations using the Lamarckian genetic algorithm local search (GALS) method. The GALS method evaluates a population of possible docking solutions and propagates the most successful individuals from each generation into the subsequent generation of possible solutions. A low-frequency local search according to the method of Solis and Wets is applied to docking trials to ensure that the final solution represents a local minimum. All dockings described in this paper were performed with a

population size of 250, and 300 rounds of Solis and Wets local search were applied with a probability of 0.06. A mutation rate of 0.02 and a crossover rate of 0.8 were used to generate new docking trials for subsequent generations, and the best individual from each generation was propagated over the next generation. The docking results from each of the 200 calculations were clustered on the basis of root-mean square deviation (rmsd) (solutions differing by less than 1.5 Å) between the Cartesian coordinates of the atoms and were ranked on the basis of free energy of binding (ΔG_{AD4}).

Compound **2b** was then built using the builder in the Maestro package of Schroedinger Suite 2007 and optimized using a version of MacroModel also included. The 4AG8 energy grids calculated for the cross-docking experiments were also used to perform AD4 calculations of **2b** employing the docking parameters described above. Because AD4 does not perform any structural optimization and energy minimization of the complexes found, a molecular mechanics/energy minimization (MM/EM) approach was applied to refine the AD4 output. The computational protocol applied consisted of the application of 100000 steps of the Polak−Ribiére conjugate gradients (PRCG) or until the derivative convergence was 0.05 kJ/mol.

Supporting Information available

Supplementary data (Tables S1a, S1b including CEREP screening results of compounds **1d**, **2b** and **2i**) associated with this article can be found in the online version.

Abbreviation used

VEGF, Vascular Endothelial Growth Factor; VEGFR, Vascular Endothelial Growth Factor Receptor; KDR, human kinase insert domain receptor; EGFR, Epidermal Growth Factor Receptor; HUVEC, human umbilical vein endothelial cell; HeLa, cervix adenocarcinoma

cell lines; A-431, epidermoid carcinoma cell lines; MSTO-211H, biphasic mesothelioma cell lines; RTK, Receptor Tyrosine Kinase.

Acknowledgment. This work was supported by MIUR (cofin 2011)

References.

[1] R.S. Kerbel, Molecular origins of cancer: Tumor angiogenesis, New Engl J Med. 358 (2008) 2039-2049.

[2] J. Folkman, Angiogenesis: an organizing principle for drug discovery?, Nat. Rev. Drug Discovery, 6 (2007) 273-286.

[3] A. Kiselyov, KV. Balakin, S.E. Tkachenko, VEGF/VEGFR signalling as a target for inhibiting angiogenesis, Expert. Opin. Inv. Drug, 16 (2007) 83-107.

[4] H. Roy, S. Bhardwaj, S. Yla-Herttuala, Biology of vascular endothelial growth factors FEBS Lett. 580 (2006) 2879-2887.

[5] R., Jr. Roskoski, VEGF receptor protein-tyrosine kinases: structure and regulation, Biochem. Biophys. Res. Commun. 375 (2008) 287−291.

[6] S. Koch, S. Tugues, X. Li, L. Gualandi, L. Claesson-Welsh, Signal transduction by vascular endothelial growth factor receptors, Biochem. J. 437 (2011) 169−183.

[7] C. H. Heldin, Dimerization of cell surface receptors in signal transduction, Cell 80 (1995) 213-223.

[8] S. R. Hubbard, M. Mohammadi, J. Schlessinger, Autoregulatory mechanisms in protein-tyrosine kinases. J. Biol. Chem. 273 (1998) 11987-11990.

[9] M. Kowanetz, N. Ferrara, Vascular endothelial growth factor signaling pathways: therapeutic perspective, Clin. Cancer Res. 12 (2006) 5018−5022.

[10] N. Ferrara, Vascular endothelial growth factor as a target for anticancer therapy, Oncologist 9 (2004) 2-10.

[11] G. Kesisis, H. Broxterman, G. Giaccone, Angiogenesis inhibitors. Drug selectivity and target specificity, Curr. Pharm. Des. 13 (2007) 2795-2809.

[12] H. Zhong, J.P. Bowen, Molecular design and clinical development of VEGFR kinase inhibitors, Curr. Top. Med. Chem. 7 (2007) 1379-1393.

[13] S. Schenone, F. Bondavalli, M. Botta, Antiangiogenic agents: an update on small molecule VEGFR inhibitors, Curr. Med. Chem. 14 (2007) 2495-2516.

[14] F. Musumeci, M. Radi, C. Brullo, S. Schenone, Vascular Endothelial Growth Factor (VEGF) Receptors: Drugs and New Inhibitors, J. Med. Chem. 55 (2012) 10797-10822.

[15] A. Da Settimo, A.M. Marini, G. Primofiore, F. Da Settimo, S. Salerno, G. Viola, L. Dalla Via, S. Marciani Magno, Synthesis, DNA binding and in vitro antiproliferative activity of purinoquinazoline, pyridopyrimidopurine and pyridopyrimidobenzimidazole derivatives as potential antitumor agents, Eur. J. Med. Chem. 33 (1998) 685-696

[16] A. Da Settimo, A.M. Marini, G. Primofiore, F. Da Settimo, S. Salerno, L. Dalla Via, O. Gia, S. Marciani Magno, Synthesis, in vitro antiproliferative activity and DNA-interaction of benzimidazoquinazoline derivatives as potential antitumor agents, Farmaco 56 (2001) 159-167.

[17] L. Dalla Via, O. Gia, S. Marciani Magno, A. Da Settimo, G. Primofiore, F. Da Settimo, F. Simorini, A. M. Marini, Dialkylaminoalkylindolonaphthyridines as potential antitumour agents: synthesis, cytotoxicity and DNA binding properties, Eur. J. Med. Chem. 37 (2002) 475-486.

[18] O.Bruno, C. Bullo, S. Schenone, F. Bondavalli, A. Ranise, M. Tognolini, M. Impicciatore, V. Ballabeni, E. Barocelli, Synthesis, antiplatelet and antithrombotic activities of new 2-substituted benzopyrano[4,3-d]pyrimidin-4-cycloamines and 4-amino/cycloamino-benzopyrano[4,3-d]pyrimidin-5-ones, Bioorg. Med. Chem. 14 (2006) 121-130, and references therein.

[19] S. Trumpp-Kallmeyer, J. R. Rubin, C. Humblet, J.M. Hamby, H.D.H. Showalter, Development of binding model to protein tyrosine kinases for substituted pyrido[2,3-d]pyrimidine inhibitors, J. Med. Chem. 41 (1998) 1752-1763.

[20] A.M. Marini, F. Da Settimo, S. Salerno, C. La Motta, F. Simorini, S. Taliani, D. Bertini, O. Gia, L. Dalla Via, Synthesis and in vitro antiproliferative activity of new substituted benzo[3',2':5,6]thiopyrano[4,3-d]pyrimidines, J. Heterocyclic Chem. 45 (2008) 745-749.

[21] J.M. Jimenez, J. Green, H. Gao, Y. Moon, G. Brenchley, R. Knegtel, F. Pierard, Preparation of aminopyrimidine derivatives as inhibitors of protein kinases. U.S. Pat. Appl. Publ. 2005, 196 pp.

[22] O. Bruno, S. Schenone, A. Ranise, F. Bondavalli, W. Filippelli, G. Falcone, G. Motola, F. Mazzeo, Antiinflammatory agents: new series of N-substituted amino acids with complex pyrimidine structures endowed with antiphlogistic activity, Farmaco 54 (1999) 95-100.

[23] S. Schenone, O. Bruno, A. Ranise, F. Bondavalli, M.L. Cenicola, C. Losasso, M. Carnevale, R. Ottavo, M. D'Antonio, ω-Dialkylaminoalkyl ethers of 6-(benzyl or phenyl)-1,3,3-trimethyl-2-oxabicyclo[2.2.2]octan-6-ol with platelet antiaggregating and local anesthetic activities, Farmaco 45 (1990) 1309-1325.

[24] S.L. Chu, W.H. Chyan, C.C. Chang, The preparation of the derivatives of 3-dialkylaminomethylthiachroman-4-ones, Huaxue Xuebao 22 (1956) 371-378.

[25] G. Primofiore, A.M. Marini, F. Da Settimo, S. Salerno, D. Bertini, L. Dalla Via, S. Marciani Magno, Synthesis of Novel 1,4-Dihydropyrido[3',2':5,6]thiopyrano[4,3-c]-pyrazoles and 5H-Pyrido[3',2':5,6]thiopyrano[4,3-d]pyrimidines as Potential Antiproliferative Agents, J. Heterocyclic Chem. 40 (2003) 783-788 and references therein.

[26] B.L. Wang, H.L. Yong, G.W. Jian, M. Yi, M.L. Zheng, Molecular design, synthesis and biological activities of amidines as new ketol-acid reductioisomerase inhibitors, Chin. Chem. Lett. 19 (2008) 651-654.

[27] R.T. Boeré, R.T. Oakley, R.W. Reed, Preparation of N,N,N'-tris(trimethylsilyl)amidines; a convenient route to unsubstituted amidines, J. Organomet. Chem. 331 (1987) 161-167.

[28] J.B. Ekeley, D.V. Tieszen, A. Ronzio, Some new amidine hydrochlorides, J. Amer. Chem. Soc. 5 (1935) 381.

[29] A.F. Crowther, F.H.S. Curd, D.N. Richardson, F.L. Rose, Synthetic antimalarials. XXIX. The preparation of some N1-aryl-N2-alkyl-N5-alkyl- and -dialkylbiguanides. J. Chem. Soc. (1948) 1636-1645.

[30] T. Nishimura, S. Tanabe, H. Toku,; T. Kono, Y. Sakabe, T. Sakaguchi, Studies on the Voges-Proskauer Reaction. I. Structure of positive substance in the diacetyl reaction, Chem. Pharm. Bull. 17 (1969) 639-649.

[31] S. Shigeya, Antistaminic Agents. III. Synthesis of N,N-dimethyl-N'-benzyl-N'-(2-pyrimidyl)ethylenediamines, Yakugaku Zasshi 72 (1952) 1444-1447.

[32] L. Yifeng, B. Yajun, Z. Juan, L. Yangyang, J. Junping, Q. Xiaoli, Optimization of the Conditions for Copper-Mediated N-Arylation of Heteroarylamines, Eur. J. Org. Chem. (2007) 6084-6088.

[33] A. Morabito, E. De Maio, M. Di Maio, N. Normanno, F. Perrone, Tyrosine Kinase Inhibitors of Vascular Endothelial Growth Factor Receptors in Clinical Trials: Current Status and Future Directions, The Oncologist, 11 (2006) 753–764.

[34] G. Bocci, A. Fioravanti, C. La Motta, P. Orlandi, B. Canu, T. Di Desidero, L. Mugnaini, S. Sartini, S. Cosconati, R. Frati, A. Antonelli, P. Berti, P. Miccoli, F. Da Settimo, R Danesi, Antiproliferative and proapoptotic activity of CLM3, a novel multiple

tyrosine kinase inhibitor, alone and in combination with SN-38 on endothelial and cancer cells. Biochem. Pharmacol. 81 (2011) 1309-1316.

[35] R.F. Nicosia, A. Ottinetti, Growth of microvessels in serum-free matrix culture of rat aorta. A quantitative assay of angiogenesis in vitro, Lab. Invest. 63 (1990) 115-122.

[36] M. J. Reed, N. Karres, D. Eyman, R.B. Vernon, Culture of murine aortic explants in 3-dimensional extracellular matrix: a novel, miniaturized assay of angiogenesis in vitro, Microvasc Res. 73 (2007) 248-252.

[37] J. Liu, F. Liu, D.L. Waller, J. Wang, Q. Liu, Kinase Inhibitors Targeting Anti-Angiogenesis as Anti-Cancer Therapies, Current Angiogenesis 1 (2012) 335-346.

[38] G.R. Zimmermann, J. Lehar, C.T. Keith, Multi-target therapeutics: when the whole is greater than the sum of the parts, Drug Discov. Today 12 (2007) 34-42.

[39] K.G. Hui, B. Seruga, J.J. Knox, Sunitinib in solid tumors, Expert Opin. Invest. Drugs, 18 (2009) 821–834.

[40] K. Hoekman, H. Van Cruijsen, G. Giaccone, The EGF(R) ana VEGR(R) pathways as combined targets for anti-angiogenesis trials in cancer therapy, in: D. Marmé, N. Fusenig (Eds.), Tumor angiogenesis basic mechanisms and Cancer therapy. Berlin, Springer, 2007, pp. 707-715.

[41] A.K. Larsen, D. Ouaret, K.El Ouadrani, A. Petitprez, Targeting EGFR and VEGR(R) pathway cross-talk in tumor survival and angiogenesis, Pharmacol. Therapeutics 131 (2011) 80-90.

[42] C. La Motta, S. Sartini, T. Tuccinardi, E. Nerini, F. Da Settimo, A. Martinelli, Computational studies of epidermal growth factor receptor: docking reliability, three-dimensional quantitative structure-activity relationship analysis, and virtual screening studies, J. Med. Chem. 52 (2009) 964-975.

[43] S. Sartini, V. Coviello, A. Bruno, V. La Pietra, L. Marinelli, F. Simorini, S. Taliani, S. Salerno, A. M. Marini, A. Fioravanti, P. Orlandi, A. Antonelli, F., Da Settimo, E. Novellino, G. Bocci, C. La Motta, Structure-based optimization of tyrosine kinase inhibitor CLM3. Design, synthesis, functional evaluation and molecular modeling studies, J. Med. Chem. 57 (2014) 1225-1235.

[44] R. Huey, G. M. Morris, A. J. Olson, D. S. Goodsell, A semiempirical free energy force field with charge–based desolvation, J. Comput. Chem. 28 (2007) 1145–1152.

[45] S. Cosconati, S. Forli, A. L. Perryman, R. Harris, D. S. Goodsell, A. J. Olson, Virtual screening with AutoDock: theory and practice, Expert Opin. Drug Discov. 5 (2010) 597–607.

[46] T. Tuccinardi, M. Botta, A. Giordano, A. Martinelli, Protein Kinases: Docking and Homology Modeling Reliability, J. Chem. Inf. Model. 50 (2010) 1432–1441.

[47] Y. Miyazaki, S. Matsunaga, J. Tang,; Y. Maeda, M. Nakano, R.J. Philippe,. M. Shibahara, W. Liu, H. Sato, L. Wang, R.T. Nolte, Novel 4-amino-furo[2,3-d]pyrimidines as Tie-2 and VEGFR2 dual inhibitors. Bioorg. Med. Chem. Lett. 15 (2005) 2203–2207.

[48] B.L. Hodous, S.D. Geuns-Meyer, P.E. Hughes, B.K. Albrecht, S. Bellon, J. Bready, S. Caenepeel, V.J. Cee, S.C. Chaffee, A. Coxon, M. Emery, J. Fretland, P. Gallant, Y. Gu, D. Hoffman, R.E. Johnson, R. Kendall, J.L Kim, A.M. Long, M. Morrison, P.R. Olivieri, V.F. Patel, A. Polverino, P. Rose, P. Tempest, L. Wang, D.A. Whittington, H. Zhao, Evolution of a highly selective and potent 2-(pyridin-2-yl)-1,3,5-triazine Tie-2 kinase inhibitor, J. Med. Chem. 50 (2007) 611–626.

[49] J.C. Harmange, M.M. Weiss, J. Germain, A.J. Polverino, G. Borg, J. Bready, D. Chen, D. Choquette, A. Coxon, T. Demelfi, L. Dipietro, N. Doerr, J. Estrada, J. Flynn, R.F. Graceffa, S.P. Harriman, S. Kaufman, D.S. La, A. Long, M.W. Martin, S. Neervannan, V.F. Patel, M. Potashman., K. Regal, P.M. Roveto, M.L. Schrag, C. Starnes, A. Tasker, Y. Teffera, L. Wang, R.D. White, D.A.Whittington, R. Zanon Naphthamides as novel and potent vascular endothelial growth factor receptor tyrosine kinase inhibitors:design, synthesis, and evaluation, J. Med. Chem. 51 (2008) 1649–1667.

[50] V.J. Cee, A.C. Cheng, K. Romero, S. Bellon, C. Mohr, D.A. Whittington, A. Bak, J. Bready, SCaenepeel, A. Coxon, H.L. Deak, J. Fretland, Y. Gu, B.L. Hodous, X. Huang, J.L. Kim, J. Lin, A.M. Long, H. Nguyen, P.R. Olivieri, V.F. Patel, L. Wang, Y. Zhou, P. Hughes, S. Geuns-Meyer, Pyridyl-pyrimidine benzimidazole derivatives as potent, selective, and orally bioavailable inhibitors of Tie-2 kinase, Bioorg. Med. Chem. Lett. 19 (2009) 424–427.

[51] Y. Oguro, N. Miyamoto, K. Okada, T. Takagi, H. Iwata, Y. Awazu, H. Miki, A. Hori, K. Kamiyama, S. Imamura, Design, synthesis, and evaluation of 5-methyl-4-phenoxy-5H-pyrrolo[3,2-d]pyrimidine derivatives: novel VEGFR2 kinase inhibitors binding to inactive kinase conformation. Bioorg. Med. Chem. 18 (2010) 7260–7273.

[52] M. Okaniwa, M. Hirose, T. Imada, T. Ohashi, Y. Hayashi, T. Miyazaki, T. Arita, M. Yabuki, K. Kakoi, J. Kato, T. Takagi, T. Kawamoto, S. Yao, A. Sumita, S. Tsutsumi, T. Tottori, H. Oki, B.C. Sang, J. Yano, K. Aertgeerts, S. Yoshida, T. Ishikawa, Design and Synthesis of Novel DFG-Out RAF/Vascular Endothelial Growth Factor Receptor 2 (VEGFR2) Inhibitors. 1. Exploration of [5,6]-Fused Bicyclic Scaffolds. J. Med. Chem. 55 (2012) 3452–3478.

[53] M. Mctigue, B.W. Murray, J.H. Chen, Y. Deng, J. Solowiej, R.S. Kania, Molecular conformations, interactions, and properties associated with drug efficiency and clinical performance among VEGFR TK inhibitors. Proc. Natl. Acad. Sci. USA, 109 (2012) 18281–18289.

[54] N. Miyamoto, N. Sakai, T. Hirayama, K. Miwa, Y. Oguro, H. Oki, K. Okada, T. Takagi, H. Iwata, Y. Awazu, S. Yamasaki, T. Takeuchi, H. Miki, A. Hori, S. Imamura, Discovery of N-[5-({2-[(cyclopropylcarbonyl)amino]imidazo[1,2-b] pyridazin-6-yl}oxy)-2-methylphenyl]-1,3-dimethyl-1H-pyrazole-5-carboxamide (TAK-593), a highly potent VEGFR2 kinase inhibitor, Bioorg. Med. Chem. 21 (2013) 2333–2345.

[55] E. F. Pettersen, T. D. Goddard, C. C. Huang, G. S. Couch, D. M. Greenblatt, E. C. Meng, T. E. Ferrin, UCSF Chimera—A Visualization System for Exploratory Research and Analysis J. Comput. Chem. 25 (2004) 1605–1612.

[56] O. Bruno, S. Schenone, A. Ranise, F. Bondavalli, E. Barocelli, V. Ballabeni, M. Chiavarini, S. Bertoni, M. Tognolini, M. Impicciatore, New polycyclic pyrimidine derivatives with antiplatelet in vitro activity: synthesis and pharmacological screening, Bioorg. Med. Chem. 9 (2001) 629-636.

[57] A. Fravolini, A. Martani, G. Grandolini, Heterocyclics from α-hydroxymethylene ketones. I. 5H-[1]Benzothiopyrano[4,3-d]pyrimidines, 4H-[1]benzothiopyrano[4,3-c]pyrazoles, and a 4H-[1]benzothiopyrano[3,4-d]isoxazole, Bollettino Scientifico della Facoltà di Chimica Industriale di Bologna 26 (1968) 269-275.